5-13-2022

A novel Chebyshev wavelet method for solving fractional-order optimal control problems

Ghodsieh Ghanbari
gg646@msstate.edu

A novel Chebyshev wavelet method for solving fractional-order optimal control problems

By

Ghodsieh Ghanbari

Approved by:

Mohsen Razzaghi (Major Professor)
Hai Dang
Seongjai Kim
Chuanxi Qian
Mohammad Sepehrifar (Committee Member/ Graduate Coordinator)
Rick Travis (Dean, College of Arts & Sciences)

A Dissertation
Submitted to the Faculty of
Mississippi State University
in Partial Fulfillment of the Requirements
for the Degree of Doctor of Philosophy
in Mathematics
in the Department of of Mathematics and Statistics

Mississippi State, Mississippi

May 2022

Name: Ghodsieh Ghanbari

Date of Degree: May 13, 2022

Institution: Mississippi State University

Major Field: Mathematics

Major Professor: Mohsen Razzaghi

Title of Study: A novel Chebyshev wavelet method for solving fractional-order optimal control problems

Pages of Study: 83

Candidate for Degree of Doctor of Philosophy

This thesis presents a numerical approach based on generalized fractional-order Chebyshev wavelets for solving fractional-order optimal control problems. The exact value of the Riemann–Liouville fractional integral operator of the generalized fractional-order Chebyshev wavelets is computed by applying regularized beta function. We apply the given wavelets, the exact formula, and collocation method to transform the studied problem to a new optimization problem. The convergence analysis of the proposed method is provided. The present method is extended for solving fractional-order, distributed-order, and variable-order optimal control problems. Illustrative examples are considered to show the advantage of this method in comparison with the existing methods in the literature.

Key words: Fractional-order Chebyshev wavelets, Numerical method, Beta function, Riemann-Liouville fractional integral operator, Fractional-order optimal control problems

DEDICATION

To my parents.

ACKNOWLEDGEMENTS

First and foremost, I would like to express my deep gratitude to my advisor, Prof. Mohsen Razzaghi, for his support, encouragement and guidance. It is truly an honor for me to have studied under his guidance. Additionally, I am very thankful to my committee members, Dr. Hai Dang, Dr. Seongjai Kim, Dr. Chuanxi Qian, and Dr. Mohammad Sepehrifar for their encouragement and support. Finally, I want to thank my family for their great support and love.

TABLE OF CONTENTS

LIST OF TABLES

LIST OF FIGURES

CHAPTER I

INTRODUCTION

Fractional calculus has gained much attention among scientists because of its vast applications in various fields such as signal processing (Gorenflo et al., 2001), solid mechanics (Rossikhin and Shitikova, 1997), mathematical finance (Ionescu et al., 2017), control theory (Bohannan, 2008), and other areas of science and engineering. Fractional-order Derivatives are generalized derivatives, which are obtained by replacing integer-order derivatives by fractional ones. A history of the development of fractional differential operators can be found in [101] and [92]. It is well known that the integer-order differential and integral operators are local, but the fractional-order differential and integral operators are non-local. When the value of an integer-order derivative at a point is computed, the obtained result depends only on that point. This property is called locality. But this is different with the fractional derivative. The fractional derivative is calculated by integrating over an entire range of values. This is main reason why differential operators of fractional order provide an excellent tool for description of memory and hereditary properties of various mathematical, physical, and engineering processes [42].

The fractional-order optimal control problems (FOCPs) are optimal control problems in which the cost function or the constraints contain fractional derivatives. FOCPs have been applied in

many areas, such as electronic, chemical, biological systems, and transportation (Hassani et al., 2019).

There are several types of fractional-order optimal control problems: distributed-order fractional optimal control problems (DO-FOCPs), variable-order fractional optimal control problems (VOFOCPs), fractional optimal control problems which contain delay argument.

In DO-FOCPS, the dynamic system contains fractional derivatives which are continuous and distributed over a given range. Some physical and engineering systems have been modeled by distributed-order differential equations. For example, these differential equations have been used to show stress relaxation in a rod [5], describe anomalous diffusion and relaxation [6], and study the rheological properties of composite materials [7].

In variable-order fractional calculus, the orders of the derivative and integral can be any given function [91]. In recent years, variable-order fractional calculus problems have been used for modeling complex systems in mathematical physics and engineering like diffusive-convective effects on the oscillatory flow [72], characterizing memory property of systems [96] (for more applications see [82, 93, 8, 7]).

In many practical problems, the behavior of the model at previous times is of important effect. A system containing the state of the model at the current time as well as the state at the previous time is called a time delay system. Time delay systems are important in many fields such as biology, medicine, chemistry, and transportation (see [3, 53] and references therein). If the FOCPs contain a delay argument, we have delay FOCPs (DFOCPs).

Due to the extensive applications of fractional calculus in engineering and science, research in this area has grown significantly, and there has been considerable interest in developing numerical

schemes for their solution, for example dynamic Hamilton–Jacobi–Bellman [81], neural networks [85], gradient-based optimization method [49], and reflection operators [21]. Over the last decade, spectral methods have emerged as one of the most efficient numerical methods for solving the dynamical systems. The key elements of the spectral method are the trial functions. The trial functions are used as the basis functions for a truncated series expansion of the solution. Orthogonal functions are usually used as trial functions [26]. The available sets of orthogonal functions can be divided into three classes. The first class includes sets of piecewise constant basis functions (e.g., block-pulse, Haar, Walsh, etc.). The second class consists of sets of orthogonal polynomials (e.g., Chebyshev, Laguerre, Legendre, etc.). The third class is the set of sine-cosine functions in the Fourier series. Orthogonal functions have been used when dealing with various problems of the dynamical systems. The main advantage of using orthogonal functions is that they reduce the dynamical system problems to those of solving a system of algebraic equations by using the operational matrices of differentiation or integration. These matrices can be uniquely determined based on the particular orthogonal functions.

Wavelets are piecewise continuous functions with compact support [0,1] and the numerical technique based on wavelets is an emerging area of research nowadays and has gained a lot of interest in many application fields, such as signal processing [25] and differential and integral equations [24]. Different variations of wavelet bases (orthogonal, biorthogonal, multiwavelets) have been presented and the design of the corresponding wavelet and scaling functions has been addressed. Wavelets permit the accurate representation of a variety of functions and operators. Moreover, wavelets establish a connection with fast numerical algorithms [13].

Due to the considerable advantages of wavelets, different types of them have been used for solving a vast area of problems. Some of these wavelets are Legendre [39], CAS [86], Bessel [26], Chebyshev [74] and Haar [50]. For these wavelets, in general, the operational matrices of integration, P^{β}, of the wavelets $\Psi(t)$ were applied in the form:

$$I^{\beta}\Psi(t) \cong P^{\beta}\Psi(t), \tag{1.1}$$

where I^{β} is the Riemann-Liouville fractional integral operator (RLFIO) of order β. To obtain P^{β}, some approximations were involved, and the values of $I^{\beta}\Psi(t)$ were not calculated exactly until 2016. To the best of our knowledge, $I^{\beta}\Psi(t)$ was calculated exactly with a hybrid of block-pulse functions and Bernoulli polynomials in [59] by using Laplace transform. Later the exact formula was obtained by applying Taylor wavelets in [99] and [102].

To obtain better accuracy, fractional-order Legendre functions, generalized Laguerre functions, and Bernoulli wavelets were introduced in [45], [16], and [75], respectively, by applying $x = t^{\alpha}$ ($\alpha > 0$). However, the RLFIO of none of these functions and wavelets was obtained exactly.

In this thesis, a new approach for solving various types of FOCPs by applying generalized fractional-order Chebyshev wavelets (GFOCW) is proposed. We give an exact formula for the RLFIO of the GFOCW and use this formula and the properties of GFOCW to solve our FOCPs. Several examples are given to illustrate the applicability and accuracy of the method. It is worth mentioning that when the exact solutions are polynomials or fractional-order power terms, we can get the exact solutions. These exact solutions were not obtained previously in the literature.

The outline of this thesis is as follows: In chapter 2, we introduce some necessary definitions and preliminaries of fractional calculus and explain some properties of generalized fractional-

order Chebyshev wavelets required for our subsequent development and we provide a formula which obtains the exact value of Riemann-Liouville fractional integral operator for generalized fractional-order Chebyshev wavelets. In chapter 3, we apply the GFOCW properties and the exact formula of the RLFIO to solve fractional-order optimal control problems (FOCPs). Moreover, the proposed method is used to find numerical solutions of FOCPs consisting inequality constraints in this chapter. The numerical approach for solving distributed-order fractional optimal control problems and variable-order fractional optimal control problems is presented in chapters 4 and 5 respectively.

CHAPTER II

PRELIMINARIES AND NOTATIONS

2.1 Generalized fractional-order Chebyshev wavelets and their properties

2.1.1 Generalized fractional-order Chebyshev wavelets

Let k be a non-negative integer and $h > 0$. For $n = 1, \ldots, 2^{k-1}$, $\hat{n} = 2n-1$ and m, a non-negative integer, the generalized Chebyshev wavelets $\psi^h_{n,m}(x)$ are defined on $[0, h]$ as [104]:

$$\psi^h_{n,m}(x) = \begin{cases} 2^{\frac{k}{2}}\,\eta_m\,U_m(2^k\,\frac{x}{h} - \hat{n}), & \text{if x} \in \left[\frac{(\hat{n}-1)h}{2^k}, \frac{(\hat{n}+1)h}{2^k}\right], \\ 0, & \text{otherwise,} \end{cases} \tag{2.1}$$

where

$$\eta_m = \begin{cases} \frac{1}{\sqrt{\pi}}, & m = 1, \\ \sqrt{\frac{2}{\pi}}, & m > 0, \end{cases} \tag{2.2}$$

and $m = 0, ..., M$. The coefficients in (2.2) make the system orthonormal. Here, $U_m(t)$ is the generalized Chebyshev polynomial of the second kind of degree m defined as follows [104]

$$U_m(x) = \sum_{j=0}^{\lfloor \frac{m}{2} \rfloor} (-1)^j \binom{m-j}{j} (2\,x)^{m-2j}. \tag{2.3}$$

A generalized fractional-order Chebyshev wavelet (GFOCW) of order α, denoted by $\psi_{n,m}^{h,\alpha}$ is obtained by setting $x = h(\frac{t}{h})^{\alpha}$ for $\alpha > 0$ over the interval $[0, h]$. So, we have:

$$\psi_{n,m}^{h,\alpha}(t) = \begin{cases} 2^{\frac{k}{2}}\,\eta_m\,U_m(2^k\,\frac{t^{\alpha}}{h^{\alpha}} - \hat{n}), & \text{if} \quad (\frac{\hat{n}-1}{2^k})^{\frac{1}{\alpha}}h \le t \le (\frac{\hat{n}+1}{2^k})^{\frac{1}{\alpha}}h, \\ 0, & \text{otherwise}, \end{cases} \tag{2.4}$$

where $n = 1, \ldots, 2^{k-1}$, and $m = 0, 1, ..., M$.

2.1.2 Function approximation based on generalized fractional-order Chebyshev wavelets

An integrable function defined over $[0, h]$, $h > 0$, can be expressed with the GFOCWs as:

$$f(t) \simeq \sum_{m=0}^{M}\sum_{n=1}^{2^{k-1}} c_{n,m}\psi_{n,m}^{h,\alpha}(t) = C^T\Psi_{k,M}^{h,\alpha}, \tag{2.5}$$

where

$$C = [c_{1,0}, ..., c_{1,M}, c_{2,0}, ..., c_{2,M}, ..., c_{2^{k-1},0}, ..., c_{2^{k-1},M}]^T, \tag{2.6}$$

and

$$\Psi_{k,M}^{h,\alpha} = [\psi_{1,0}^{h,\alpha}, ..., \psi_{1,M}^{h,\alpha}, \psi_{2,0}^{h,\alpha}, ..., \psi_{2,M}^{h,\alpha}, ..., \psi_{2^{k-1},0}^{h,\alpha}, ..., \psi_{2^{k-1},M}^{h,\alpha}]^T. \tag{2.7}$$

2.2 The fractional derivative and integral

There are several definitions of fractional derivative and integration. The commonly used definitions for fractional derivative and fractional integration are the Caputo definition and the Riemann-Liouville definition respectively.

Here, by $C[0, h]$, we denote the set of all continuous real valued functions defined over the interval $[0, h]$. In addition, we use $C^n[0, h]$ to denote the set of all n-times continuously differentiable functions in $C[0, h]$.

Definition 1

The Riemann-Liouville fractional integral operator (*RLFIO*) *of order* $\beta \geq 0$ *of a function* $f(x)$ *in* $C[0,h]$ *is defined as* [63]

$$I^{\beta} f(x) = \begin{cases} \frac{1}{\Gamma(\beta)} \int_0^x f(s)(x-s)^{\beta-1} ds, & \beta > 0, \\ \\ f(x), & \beta = 0. \end{cases}$$

Definition 2

The Caputo fractional derivative operator of order $\beta \geq 0$ *of* $f(x)$ *in* $C^n[0,h]$ *is defined as* [63]:

$$D^{\beta} f(x) = \begin{cases} \frac{1}{\Gamma(n-\beta)} \int_0^x f^{(n)}(s)\,(x-s)^{n-\beta-1}\, ds, & 0 \leq n-1 < \beta \leq n \in \mathbb{N}, \\ \\ f^{(n)}(x), & \beta = n \in \mathbb{N}. \end{cases} \tag{2.8}$$

Proposition 1. The operators I^{β} and D^{β} are linear operators and they satisfy the following properties:

1. $I^{\beta} D^{\beta} f(x) = f(x) - \sum_{k=0}^{n-1} f^{(k)}(0) \frac{x^k}{k!}, \quad$ if $x \geq 0$.
2. $I^{\beta} x^{\alpha} = \frac{\Gamma(\alpha+1)}{\Gamma(\alpha+\beta+1)} x^{\alpha+\beta}$, for every real number $\alpha > -1$.
3. $D^{\beta} x^{\alpha} = \frac{\Gamma(\alpha+1)}{\Gamma(\alpha-\beta+1)} x^{\alpha-\beta}$, for every real number $\alpha > \beta - 1$.
4. $D^{\beta} I^{\beta} f(x) = f(x)$.
5. $D^{\beta_2} I^{\beta_1} f(x) = I^{\beta_1-\beta_2} f(x), \quad$ for $\beta_1 \geq \beta_2$.

2.3 Error bounds

In this section, the error bound of the function approximation and fractional derivative and integral are presented.

The Sobolev norm of order $\xi \geq 0$ of a function over the interval $(0, 1)$ is defined by [18]

$$\|f\|_{H^{\xi}(0,1)} = \left(\sum_{k=0}^{\xi} \int_0^1 |f^{(k)}(t)|^2 dt \right)^{\frac{1}{2}} = \left(\sum_{k=0}^{\xi} \|f^{(k)}(t)\|^2_{L^2(0,1)} \right)^{\frac{1}{2}}, \tag{2.9}$$

where $f^{(k)}$ is the kth derivative of f, and $H^{\xi}(0, 1)$ denotes the Hilbert space. In addition,

$$|f|_{H^{\xi;M}(0,1)} = \left(\sum_{k=min(\xi,M+1)}^{\xi} \|f^{(k)}(t)\|^2_{L^2(0,1)} \right)^{\frac{1}{2}},$$

$$|f|_{H^{r;\xi;M;N}(0,1)} = \left(\sum_{k=min(\xi,M+1)}^{\xi} N^{2r-2k} \|f^{(k)}(t)\|^2_{L^2(0,1)} \right)^{\frac{1}{2}}.$$

2.3.1 Error bound for the function approximation

The following theorem gives the error bound for approximating a function by GFOCWs.

Theorem 1

Suppose $f \in H^{\xi}(0, 1)$ with $\xi \geq 0$, and $P_M^{2^{k-1}} f$ is the best approximation of f out of $\Psi_{k,M}^{h,\alpha}$ then [77]

$$\|f - P_M^{2^{k-1}} f\|_{L^2(0,1)} \leq cM^{-\xi}(2^{k-1})^{-\xi} \|f^{(\xi)}\|_{L^2(0,1)}, \tag{2.10}$$

and for $1 \leq r \leq \xi$

$$\|f - P_M^{2^{k-1}} f\|_{H^{\xi}(0,1)} \leq cM^{2r-\frac{1}{2}-\xi}(2^{k-1})^{r-\xi} \|f^{(\xi)}\|_{L^2(0,1)}, \tag{2.11}$$

where c depends on ξ.

Theorem 2

Suppose $f \in H^{\xi}(0,1)$ *with* $\xi \geq 0$*, and* $0 < \mu \leq 1$*, then*

$$\|D^{\mu} f - D^{\mu}(P_M^{2^{k-1}} f)\|_{L^2(0,1)} \leq \frac{1}{\Gamma(2-\mu)} c M^{2r-\frac{1}{2}-\xi} (2^{k-1})^{r-\xi} \|f^{(\xi)}\|_{L^2(0,1)}, \tag{2.12}$$

where $1 \leq r < \xi$.

Proof: By applying properties of the RLFIO, Caputo fractional derivative operator, and [12]

$$\|f * h\|_p \leq \|f\|_1 \|h\|_p,$$

we have

$$\begin{aligned}
\|D^{\mu} f - D^{\mu}(P_{M-1}^{2^{k-1}} f)\|_{L^2(0,1)}^2 &= \|I^{1-\mu}(D^1 f - D^1(P_{M-1}^{2^{k-1}} f))\|_{L^2(0,1)}^2 \\
&= \|\frac{1}{t^{\mu}\,\Gamma(1-\mu)} * (D^1 f - D^1(P_{M-1}^{2^{k-1}} f)\|_{L^2(0,1)}^2 \\
&\leq \left(\frac{1}{(1-\mu)\Gamma(1-\mu)}\right)^2 \|D^1 f - D^1(P_{M-1}^{2^{k-1}} f)\|_{L^2(0,1)}^2 \\
&\leq \left(\frac{1}{\Gamma(2-\mu)}\right)^2 \|f - P_{M-1}^{2^{k-1}} f\|_{H^r(0,1)}^2 \\
&\leq \left(\frac{1}{\Gamma(2-\mu)}\right)^2 c^2 (M-1)^{4r-1-2\xi} (2^{k-1})^{2r-2\xi} \|f^{(\xi)}\|_{L^2(0,1)}^2. \qquad (2.13)
\end{aligned}$$

Taking the square root of Eq. (2.13), gives us Eq. (2.12). ∎

Theorem 3

Suppose $f \in H^{\xi}(0,1)$ *with* $\xi \geq 0$*, and* $\mu \geq 0$*, then* [60]

$$\|I^{\beta} f - I^{\beta}(P_{M-1}^{2^{k-1}} f)\|_{L^2(0,1)}^2 \leq \frac{1}{\Gamma(\beta)} c M^{-\xi} 2^{-(k-1)\xi} \|f^{(\xi)}\|_{L^2(0,1)}. \tag{2.14}$$

Proof: By using Definition 1, we get

$$\|I^{\beta}f(x) - I^{\beta}(P_{M-1}^{2^{k-1}}f(x))\|_{L^2(0,1)}^2 = \|\frac{1}{\Gamma(\beta)}\int_0^x (x-s)^{\beta-1}(f(s) - P_{M-1}^{2^{k-1}}f(s))ds\|_{L^2(0,1)},$$

$$\leq \|\frac{1}{\Gamma(\beta)}\int_0^1 (1-s)^{\beta-1}((f(s) - P_{M-1}^{2^{k-1}}f(s))ds\|_{L^2(0,1)},$$

$$\leq \|\frac{1}{\Gamma(\beta)}\int_0^1 \|f(s) - P_{M-1}^{2^{k-1}}f(s))ds\|_{L^2(0,1)},$$

from Equation (2.10), we obtain Equation (2.14). ∎

2.4 Riemann-Liouville fractional integral operator for GFOCW

In this section, we provide an exact formula for computing the RLFIO of the GFOCW. To this end, we use the unit step function,

$$\mu_c(x) = \begin{cases} 1, & \text{if} \qquad x \geq c, \\ 0, & \qquad \text{otherwise.} \end{cases}$$

The regularized beta function is given in [1] by

$$\mathbf{I}(x;a,b) = \frac{1}{B(a,b)}\int_0^x s^{a-1}(1-s)^{b-1}ds,$$

where $B(a,b) = \frac{\Gamma(a)\Gamma(b)}{\Gamma(a+b)}$ is the beta function.

Lemma 1

Let $c \geq 0$ and $\alpha \geq 0$. Then, for a real number $\beta > 0$, we have

$$I^{\beta}\left(x^{\alpha}\mu_c(x)\right) = \frac{\Gamma(\alpha+1)}{\Gamma(\alpha+\beta+1)}x^{\alpha+\beta}\left[1 - \mathbf{I}\left(\frac{c}{x};\alpha+1,\beta\right)\right]\mu_c(x). \tag{2.15}$$

Proof: For $0 \leq x < c$, both sides of Eq. (2.15) are equal to zero. For $x \geq c$, by using the definition of the unit step function, we have

$$\begin{aligned} I^{\beta}\left(x^{\alpha}\mu_c(x)\right) &= \frac{1}{\Gamma(\beta)}\int_0^x s^{\alpha}\mu_c(s)(x-s)^{\beta-1}ds \\ &= \frac{1}{\Gamma(\beta)}\int_0^x s^{\alpha}(x-s)^{\beta-1}ds - \frac{1}{\Gamma(\beta)}\int_0^c s^{\alpha}(x-s)^{\beta-1}ds \\ &= I^{\beta}(x^{\alpha}) - \frac{x^{\alpha+\beta}}{\Gamma(\beta)}\int_0^c \left(\frac{s}{x}\right)^{\alpha}\left(1-\frac{s}{x}\right)^{\beta-1} d\left(\frac{s}{x}\right) \\ &= \frac{\Gamma(\alpha+1)}{\Gamma(\alpha+\beta+1)}x^{\alpha+\beta}\left(1 - \frac{\Gamma(\alpha+\beta+1)}{\Gamma(\alpha+1)\Gamma(\beta)}\int_0^{\frac{c}{x}} t^{\alpha}(1-t)^{\beta-1}\,dt\right). \end{aligned}$$

Therefore, we get

$$I^{\beta}\left(x^{\alpha}\mu_c(x)\right) = \frac{\Gamma(\alpha+1)}{\Gamma(\alpha+\beta+1)}x^{\alpha+\beta}\left[1 - \mathbf{I}\left(\frac{c}{x};\alpha+1,\beta\right)\right]\mu_c(x).$$

■

Theorem 4

For $\alpha, \beta > 0$, we have

$$I^{\beta}\psi_{n,m}^{h,\alpha}(t) = \begin{cases} 0, & \text{if } t < c_1, \\ U(t), & \text{if } c_1 \leq t < c_2, \\ U(t) - V(t), & \text{if } t \geq c_2, \end{cases} \tag{2.16}$$

where

$$\begin{aligned} U(t) &= 2^{\frac{k}{2}}\eta_m \sum_{j=0}^{\lfloor \frac{m}{2} \rfloor}(-1)^j \binom{m-j}{j} \sum_{r=0}^{m-2j}\binom{m-2j}{r}\frac{2^{r(k+1)}}{h^{\alpha r}}(-2\hat{n})^{m-2j-r} \\ &\quad \times \frac{\Gamma(\alpha r+1)}{\Gamma(\alpha r+1+\beta)}t^{\alpha r+\beta} \times \left[1 - \mathbf{I}\left(\frac{c_1}{t};\alpha r+1,\beta\right)\right], \end{aligned}$$

$$V(t) = 2^{\frac{k}{2}}\,\eta_m \sum_{j=0}^{\lfloor \frac{m}{2} \rfloor}(-1)^j \binom{m-j}{j} \sum_{r=0}^{m-2j} \binom{m-2j}{r} \frac{2^{r(k+1)}}{h^{\alpha r}}(-2\hat{n})^{m-2j-r} \times \frac{\Gamma(\alpha r+1)}{\Gamma(\alpha r+1+\beta)} t^{\alpha r+\beta} \times \left[1 - \mathbf{I}\left(\frac{c_2}{t}; \alpha r+1, \beta\right)\right],$$

and

$$c_1 = h\left(\frac{\hat{n}-1}{2^k}\right)^{\frac{1}{\alpha}},\ c_2 = h\left(\frac{\hat{n}+1}{2^k}\right)^{\frac{1}{\alpha}}.$$

Proof: By using the unit step functions, we have

$$\mu_{c_1}(t) - \mu_{c_2}(t) = \begin{cases} 1, & \text{if } c_1 \le t < c_2, \\ \\ 0, & \text{otherwise.} \end{cases}$$

Therefore, the GFOCW can be rewritten as

$$\begin{aligned}
\psi_{n,m}^{h,\alpha}(t) &= 2^{\frac{k}{2}}\,\eta_m\, U_m(2^k \frac{t^\alpha}{h^\alpha} - \hat{n})\left(\mu_{c_1}(t) - \mu_{c_2}(t)\right) \\
&= 2^{\frac{k}{2}}\,\eta_m \sum_{j=0}^{\lfloor \frac{m}{2} \rfloor}(-1)^j \binom{m-j}{j} (2^{k+1}\frac{t^\alpha}{h^\alpha} - 2\hat{n})^{m-2j}\left(\mu_{c_1}(t) - \mu_{c_2}(t)\right) \\
&= 2^{\frac{k}{2}}\,\eta_m \sum_{j=0}^{\lfloor \frac{m}{2} \rfloor}(-1)^j \binom{m-j}{j} \sum_{r=0}^{m-2j} \binom{m-2j}{r} (2^{k+1}\frac{t^\alpha}{h^\alpha})^r (-2\hat{n})^{m-2j-r}\left(\mu_{c_1}(t) - \mu_{c_2}(t)\right) \\
&= 2^{\frac{k}{2}}\,\eta_m \sum_{j=0}^{\lfloor \frac{m}{2} \rfloor}(-1)^j \binom{m-j}{j} \sum_{r=0}^{m-2j} \binom{m-2j}{r} \frac{2^{(k+1)r}}{h^{\alpha r}} t^{\alpha r}(-2\hat{n})^{m-2j-r}\left(\mu_{c_1}(t) - \mu_{c_2}(t)\right).
\end{aligned}$$

Therefore,

$$I^\beta\left(\psi_{n,m}^{h,\alpha}(t)\right) = 2^{\frac{k}{2}}\,\eta_m \sum_{j=0}^{\lfloor \frac{m}{2} \rfloor}(-1)^j \binom{m-j}{j} \sum_{r=0}^{m-2j} \binom{m-2j}{r} \frac{2^{(k+1)r}}{h^{\alpha r}}(-2\hat{n})^{m-2j-r} \times \left[I^\beta\left(t^{\alpha r}\mu_{c_1}(t)\right) - I^\beta\left(t^{\alpha r}\mu_{c_2}(t)\right)\right].$$

From Eq. (2.15) in Lemma 1, we have

$$
\begin{aligned}
I^{\beta}\left(\psi_{n,m}^{h,\alpha}(t)\right) = \quad & 2^{\frac{k}{2}}\,\eta_m \sum_{j=0}^{\lfloor \frac{m}{2} \rfloor} (-1)^j \binom{m-j}{j} \sum_{r=0}^{m-2j} \binom{m-2j}{r} \frac{2^{(k+1)r}}{h^{\alpha r}} (-2\hat{n})^{m-2j-r} \\
& \times \left[\frac{\Gamma(\alpha r+1)}{\Gamma(\alpha r+1+\beta)} t^{\alpha r+\beta} \left(1 - \mathbf{I}\left(\frac{c_1}{t}; \alpha r+1, \beta\right)\right) \mu_{c_1}(t) \right. \\
& \left. - \frac{\Gamma(\alpha r+1)}{\Gamma(\alpha r+1+\beta)} t^{\alpha r+\beta} \left(1 - \mathbf{I}\left(\frac{c_2}{t}; \alpha r+1, \beta\right)\right) \mu_{c_2}(t) \right].
\end{aligned}
$$

By setting

$$
\begin{aligned}
U(t) &= 2^{\frac{k}{2}}\,\eta_m \sum_{j=0}^{\lfloor \frac{m}{2} \rfloor} (-1)^j \binom{m-j}{j} \sum_{r=0}^{m-2j} \binom{m-2j}{r} \frac{2^{(k+1)r}}{h^{\alpha r}} (-2\hat{n})^{m-2j-r} \\
&\quad \times \frac{\Gamma(\alpha r+1)}{\Gamma(\alpha r+1+\beta)} t^{\alpha r+\beta} \times \left[1 - \mathbf{I}\left(\frac{c_1}{t}; \alpha r+1, \beta\right)\right],
\end{aligned}
$$

and

$$
\begin{aligned}
V(t) &= 2^{\frac{k}{2}}\,\eta_m \sum_{j=0}^{\lfloor \frac{m}{2} \rfloor} (-1)^j \binom{m-j}{j} \sum_{r=0}^{m-2j} \binom{m-2j}{r} \frac{2^{(k+1)r}}{h^{\alpha r}} (-2\hat{n})^{m-2j-r} \\
&\quad \times \frac{\Gamma(\alpha r+1)}{\Gamma(\alpha r+1+\beta)} t^{\alpha r+\beta} \times \left[1 - \mathbf{I}\left(\frac{c_2}{t}; \alpha r+1, \beta\right)\right],
\end{aligned}
$$

we obtain Eq. (2.16). ∎

CHAPTER III

FRACTIONAL-ORDER OPTIMAL CONTROL PROBLEMS

The focus of this chapter is on solving fractional optimal control problems (FOCPs). Different definitions of fractional derivatives can be used to define FOCPs. The widely used one are Riemann-Liouville and Caputo fractional derivatives. The Hamiltonian formulation for FOCPs was studied in [14] and [2]. Several numerical schemes have been applied to solve FOCPs, for example, Legendre wavelets [39], Chelyshkov polynomials [40], dynamic Hamilton–Jacobi–Bellman [81], modified hat functions [68], neural networks [85], Hermite polynomials [106], Laguerre polynomials [94], gradient-based optimization method [49], Chebyshev wavelets [55], and reflection operators [21]. We apply GFOCW and its properties to solve these problems.

3.1 Problem statement and numerical method

We consider FOCP as

$$min \quad J(x,u) = \int_0^1 f\,(t, x(t), u(t))\; dt, \tag{3.1}$$

subject to

$$u(t) = G(t, x(t), D^{\beta_0}x(t), D^{\beta_1}x(t), ..., D^{\beta_r}x(t)), \tag{3.2}$$

and

$$x^{(k)}(0) = \lambda_k, \quad k = 0, 1, 2, ..., n-1, \tag{3.3}$$

where $\beta_0 \geq \beta_1 \geq ... \geq \beta_r$, and $n-1 < \beta_0 \leq n$, for $n \in \mathbb{N}$.

First, we expand $D^{\beta_0}x(t)$ by using GFOCW:

$$D^{\beta_0}x(t) \simeq C^T \Psi^{h,\alpha}_{k,M}(t), \tag{3.4}$$

where C, and $\Psi^{h,\alpha}_{k,M}(t)$ are defined in Eqs. (2.6) and (2.7) respectively. Then by applying the operator I^{β_0} to Eq. (3.4), we obtain

$$x(t) \simeq C^T I^{\beta_0} \Psi^{h,\alpha}_{k,M}(t) + \sum_{k=0}^{n-1} \frac{\lambda_k}{k!} t^k, \tag{3.5}$$

where $\beta_0 \leq n$. For each $i = 1, \ldots, r$, by applying the operator D^{β_i} to Eq. (3.5) and using Proposition 1, we obtain

$$\begin{aligned} D^{\beta_i}x(t) &\simeq C^T I^{\beta_0-\beta_i} \Psi^{h,\alpha}_{k,M}(t) + \sum_{k=0}^{n-1} \frac{\lambda_k}{k!} D^{\beta_i}(t^k) \\ &= C^T I^{\beta_0-\beta_i} \Psi^{h,\alpha}_{k,M}(t) + \sum_{k=\lceil \beta_i \rceil}^{n-1} \frac{\lambda_k}{\Gamma(k-\beta_i+1)} t^{k-\beta_i}. \end{aligned} \tag{3.6}$$

Here

$$\begin{aligned} I^{\beta_0} \Psi^{h,\alpha}_{k,M}(t) = \Big[& I^{\beta_0}\psi^{h,\alpha}_{1,0}(t), \ldots, I^{\beta_0}\psi^{h,\alpha}_{1,M}(t), I^{\beta_0}\psi^{h,\alpha}_{2,0}(t), \ldots, I^{\beta_0}\psi^{h,\alpha}_{2,M}(t), \ldots, \\ & I^{\beta_0}\psi^{h,\alpha}_{2^{k-1},0}(t), \ldots, I^{\beta_0}\psi^{h,\alpha}_{2^{k-1},M}(t) \Big]. \end{aligned}$$

By substituting Eqs. (3.4)-(3.6) in Eq. (3.2), we get

$$u(t) \simeq G\left(t,\, C^T I^{\beta_0} \Psi^{h,\alpha}_{k,M}(t) + \sum_{k=0}^{n-1} \frac{\lambda_k}{k!} t^k,\, C^T \Psi^{h,\alpha}_{k,M}(t), ..., C^T I^{\beta_0-\beta_r} \Psi^{h,\alpha}_{k,M}(t) + \sum_{k=\lceil \beta_r \rceil}^{n-1} \frac{\lambda_k}{\Gamma(k-\beta_r+1)} t^{k-\beta_r} \right). \tag{3.7}$$

By applying Eqs. (3.5) and (3.7) in Eq. (3.1), we have

$$J = J(x,u) = \int_0^1 f\left(t, C^T\ I^{\beta_0}\Psi^{h,\alpha}_{k,M}(t) + \sum_{k=0}^{n-1}\frac{\lambda_k}{k!}t^k, G\left(t, C^T I^{\beta_0}\Psi^{h,\alpha}_{k,M}(t)\right.\right.$$
$$\left.\left. + \sum_{k=0}^{n-1}\frac{\lambda_k}{k!}t^k,\ C^T\Psi^{h,\alpha}_{k,M}(t), ..., C^T I^{\beta_0-\beta_r}\Psi^{h,\alpha}_{k,M}(t) + \sum_{k=\lceil\beta_r\rceil}^{n-1}\frac{\lambda_k}{\Gamma(k-\beta_r+1)}t^{k-\beta_r}\right)\right)dt. \tag{3.8}$$

Next, we evaluate the integral in Eq. (3.8) numerically by using Gauss-Legendre quadrature. For the error of the Gauss-Legendre quadrature method, please refer to Chapter 19 of [100]. According to differential calculus, we have the following necessary conditions for optimizing the cost functional J given in Eq. (3.8) [78]

$$\frac{\partial J}{\partial c_{nm}} = 0, \quad 1 \le n \le 2^{k-1},\ 0 \le m \le M.$$

To find the unknown constants c_{nm}, we will solve the above nonlinear algebraic system by using Newton's iterative method. It is well-known that the initial guess for Newton's iteration method is very important, especially for a complicated problem [58]. The initial guess in this case can be obtained similarly to the method given in [108]. By evaluating C, the optimal control $u(t)$ can be calculated.

3.2 Illustrative examples

In this section, we compare our numerical method with several existing methods in the literature. Our numerical solutions were calculated by using Mathematica 12.1.1. We consider the examples for which the integral in the cost functional is defined over the interval $[0, 1]$. However, if we have the integral defined over $[0, h]$, since GFOCW given in Eq. (2.4) is defined over $[0, h]$, we can change the interval for the integral to the interval $[0, 1]$ by using appropriate transformation.

For the first two given examples, the present method can obtain the exact solutions while the other existings methods could not obtain these exact solutions.

Example 3.2.1. We consider the following FOCP [90]

$$min \quad J(x,u) = \frac{1}{2}\int_0^1 \left[\left(x(t) - t^\beta\right)^2 + \left(u(t) - t^\beta - \Gamma(\beta+1)\right)^2\right] dt, \tag{3.9}$$

subject to

$$D^\beta x(t) = -x(t) + u(t), \quad \text{and} \;\; x(0) = 0. \tag{3.10}$$

The optimal state and control functions are $x(t) = t^\beta$, and $u(t) = t^\beta + \Gamma(\beta+1)$, with corresponding minimum cost functional $J_{opt} = 0$.

This FOCP was solved in [90] by using the Legendre wavelet method (LWM), Laguerre wavelet method (LaWM), and Chebyshev wavelet method (CWM) with $k = 1$, $M_1 = 4, \beta = 1$, and 0.5. Here M_1 is the degree of the polynomials used in these wavelets. We solve this problem in two cases: $\beta = 1$ and $\beta = 0.5$ with $\alpha = \beta$, $k = 1$ and $M = 2$.

For $\beta = 1$, we expand $D^\beta x(t)$ by GFOCW as follows:

$$D^\beta x(t) = C^T \Psi_{1,2}^{1,1}(t), \tag{3.11}$$

where

$$\Psi_{1,2}^{1,1}(t) = \left[\sqrt{\frac{2}{\pi}}, \frac{-4+8t}{\sqrt{\pi}}, \frac{6-32t+32t^2}{\sqrt{\pi}}\right]^T. \tag{3.12}$$

Then,

$$x(t) = C^T I^\beta \Psi_{1,2}^{1,1}(t), \tag{3.13}$$

where

$$I^\beta \Psi_{1,2}^{1,1}(t) = \left[\sqrt{\frac{2}{\pi}}\, t, \frac{4t(t-1)}{\sqrt{\pi}}, \frac{2t(3-4t)^2}{3\sqrt{\pi}}\right]^T. \tag{3.14}$$

Now, by substituting Eqs. (3.11) and (3.13) in Eq. (3.10), we get

$$u(t) = C^T \Psi_{1,2}^{1,1}(t) + C^T I^{\beta} \Psi_{1,2}^{1,1}(t). \tag{3.15}$$

By substituting Eqs. (3.13) and (3.15) in Eq. (3.9), we get a parameter optimization problem. By solving this problem, we obtain the unknown parameter $C = \left[\sqrt{\frac{\pi}{2}}, 0, 0\right]^T$. By using Eqs. (3.9), (3.13) and (3.15), we get $x(t) = t, u(t) = 1 + t$, and $J = 0$, which are the exact solutions. These solutions were not obtained in [90] for any of the wavelets used for this example.

For $\beta = 0.5$, by using the similar argument, we get $C = \left[\frac{\pi}{2\sqrt{2}}, 0, 0\right]^T$. For this case, we obtain $x(t) = t^{\frac{1}{2}}$, and $u(t) = t^{\frac{1}{2}} + \frac{1}{2}\sqrt{\pi}$ which are the exact solutions. Again, these exact solutions were not obtained in [90].

Example 3.2.2. Consider the following FOCP [26]

$$min \quad J(x,u) = \int_0^1 (u(t) - x(t))^2 \, dt, \tag{3.16}$$

subject to

$$\dot{x}(t) + D^{\beta} x(t) = u(t) - x(t) + t^3 + \frac{6\, t^{\beta+2}}{\Gamma(\beta+3)}, \quad 0 < \beta \leq 1, \tag{3.17}$$

with $x(0) = 0$. The optimal solutions are $x(t) = u(t) = \frac{6\, t^{\beta+3}}{\Gamma(\beta+4)}$, with the corresponding optimal cost functional $J = 0$.

In case $\beta = 1$, we expand $D^{\beta} x(t)$ by GFOCW as follows:

$$D^{\beta} x(t) = C^T \Psi_{1,3}^{1,1}(t). \tag{3.18}$$

Then,

$$x(t) = C^T I^{\beta} \Psi_{1,3}^{1,1}(t). \tag{3.19}$$

Now, by substituting Eqs. (3.18) and (3.19) in Eq. (3.17), we get

$$u(t) = 2C^T\Psi_{1,3}^{1,1}(t) + C^T I^{\beta}\Psi_{1,3}^{1,1}(t) - t^3 - \frac{6\,t^{\beta+2}}{\Gamma(\beta+3)}. \tag{3.20}$$

By substituting Eqs. (3.19) and (3.20) in Eq. (3.16), we get

$$J = \int_0^1 \left(2C^T\Psi_{1,3}^{1,1}(t) + C^T I^{\beta}\Psi_{1,3}^{1,1}(t) - t^3 - \frac{6\,t^{\beta+2}}{\Gamma(\beta+3)} - C^T I^{\beta}\Psi_{1,3}^{1,1}(t)\right)^2 dt. \tag{3.21}$$

The given problem is now reduced to the following parameter optimization problem: Finding the unknown constants C, which minimize the cost functional J given in Eq. (3.21). By solving the latter problem, we obtain the unknown constants as $C = \left[\frac{7\sqrt{\pi/2}}{32}, \frac{7\sqrt{\pi}}{64}, \frac{3\sqrt{\pi}}{64}, \frac{\sqrt{\pi}}{128}\right]^T$, which gives the exact solutions $x(t) = u(t) = \frac{t^4}{4}$, and the minimal cost $J = 0$.

In case $\beta = 0.5$, we solve with $\alpha = 0.5$, $k = 1$, and $M = 5$. We obtain the unknown constants as

$$C = \left[\frac{33}{80\sqrt{2}}, \frac{33}{128}, \frac{11}{64}, \frac{11}{160}, \frac{1}{64}, \frac{1}{640}\right]^T.$$

From the above equation, we obtain $x(t) = u(t) = \frac{6x^{3.5}}{\Gamma(4.5)}$, and the minimal cost $J = 0$, which are the exact solutions. This problem has been solved in [26] by applying Bessel wavelets and in [73] by using Bernoulli polynomials. These exact solutions were not obtained in [26] and [73].

For the cases when $\beta = 0.8, 0.9$, we solve with $\alpha = k = 1$ and $M = 5$. We compare the absolute errors for the obtained $x(t)$, $u(t)$, and J with those from the Bessel wavelet method with $k = 1$, $M_2 = 5$ reported in [26] in Table 3.1 on page 33, Table 3.2 on page 34, and Table 3.3 on page 34, respectively. Here, M_2 is the degree of the Bessel polynomials. It is noted that, since we get the exact value for $x(t)$ with $\beta = 1, k = 1, M = 5$, the column for $\beta = 1$ in Table 3.2.2.1 is all equal to zero.

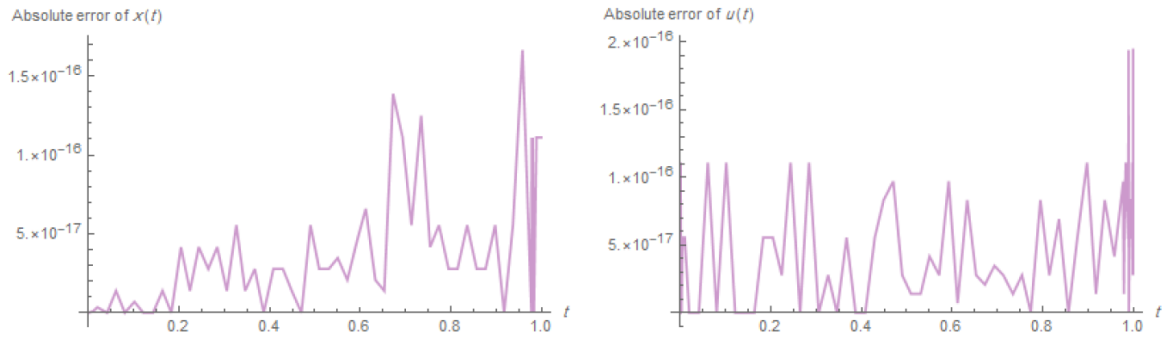

Figure 3.1

Graphs of absolute error functions of x(t) and u(t) for $\alpha = 0.5$, $\beta = 1$, $k = 1$, and $M = 2$ for Example 3.2.3

Example 3.2.3. Consider the following FOCP [26]

$$min \quad J(x,u) = \int_0^1 \left(\left(x(t) - t^2 \right)^2 + \left(u(t) - te^{-t} + \frac{1}{2} e^{t^2 - t} \right)^2 \right) dt, \tag{3.22}$$

subject to

$$D^{\beta} x(t) = e^{x(t)} + 2e^{t} u(t), \quad x(0) = 0, \quad 0 < \beta \leq 1. \tag{3.23}$$

When $\beta = 1$, the optimal solutions are $x(t) = t^2$ and $u(t) = te^{-t} - \frac{1}{2} e^{t^2 - t}$ with the corresponding optimal cost functional $J = 0$. We solve this problem for $\alpha = 0.5$, $k = 1$, and $M = 2$. In Table 3.4 on page 35, we compare the obtained numerical results using our method with those obtained by the Bessel wavelet method with $M_2 = 5$ in [26]. Figure 3.1 represents graphs of absolute error functions of x(t) and u(t) obtained by the present method for $\alpha = 0.5$, $\beta = 1$, $k = 1$, and $M = 2$.

Example 3.2.4. Consider the following FOCP [11]

$$min \quad J = \int_0^1 \left(\left(x(t) - t^2 \right)^2 + \left(u(t) + t^4 - \frac{20\, t^{0.9}}{9\Gamma(0.9)} \right)^2 \right) dt,$$

subject to

$$D^{1.1}x(t) = u(t) + t^2x(t),$$

$$x(0) = \dot{x}(0) = 0.$$

The optimal cost functional value is $J = 0$, which is obtained by

$$x(t) = t^2, \quad and \quad u(t) = \frac{20\,t^{0.9}}{9\Gamma(0.9)} - t^4.$$

This problem has been solved in [11] by applying Bernoulli wavelets. Table 3.5 on page 36 and Table 3.6 on page 36 provide comparisons between our method with $\beta = \alpha = 1$, $k = 2$ and Bernoulli wavelets for $\beta = 1$, $k = 2$, and different values of M and M_4. Here, M_4 is the degree of Bernoulli polynomials. As M increases for the same k, the error of J in Table 3.5 on page 36 tends to zero. In addition, Table 3.6 on page 36 also suggests that as M increases for the same k, the errors of x(t) and u(t) decrease.

Example 3.2.5. Consider the following FOCP [11]

$$min \quad J(x_1, x_2, u) = 0.5 \int_0^1 \left(x_1^2(t) + x_2^2(t) + u^2(t)\right) dt, \tag{3.24}$$

subject to

$$D^{\beta}x_1(t) = u(t) - x_1(t) + x_2(t), \tag{3.25}$$

$$D^{\beta}x_2(t) = -2\,x_2(t), \tag{3.26}$$

with $x_1(0) = x_2(0) = 1$.

For $\beta = 1$, the optimal cost functional value is $J = 0.4319835548817479$ which is obtained by

$$x_1(t) = \frac{-3}{2}e^{-2t} + 2.48164\, e^{-\sqrt{2}t} + 0.018352\, e^{\sqrt{2}t},$$

$$x_2(t) = e^{-2t},$$

$$u(t) = \frac{1}{2}e^{-2t} - 1.02793\, e^{-\sqrt{2}t} + 0.0443056\, e^{\sqrt{2}t}.$$

To solve this problem, we expand $D^\beta x_1(t)$ and $D^\beta x_2(t)$ by GFOCW as follows:

$$D^\beta x_1(t) = C^T \Psi^{h,\alpha}_{k,M}(t), \tag{3.27}$$

$$D^\beta x_2(t) = E^T \Psi^{h,\alpha}_{k,M}(t), \tag{3.28}$$

where C and E are given in Eq. (2.6), and $\Psi^{h,\alpha}_{k,M}(t)$ in Eq. (2.7). Then

$$x_1(t) = C^T I^\beta \Psi^{h,\alpha}_{k,M}(t) + 1, \tag{3.29}$$

$$x_2(t) = E^T I^\beta \Psi^{h,\alpha}_{k,M}(t) + 1. \tag{3.30}$$

By substituting Eqs. (3.27)–(3.30) to Eq. (3.25), we have

$$u(t) = C^T \Psi^{h,\alpha}_{k,M}(t) + C^T I^\beta \Psi^{h,\alpha}_{k,M}(t) + 1 - \left(E^T I^\beta \Psi^{h,\alpha}_{k,M}(t) + 1\right). \tag{3.31}$$

Then, we substitute Eqs. (3.29)–(3.31) in the cost functional J in Eq. (3.24), and Eqs. (3.28) and (3.30), in Eq. (3.26). Hence, we get

$$J(x_1, x_2, u) = 0.5 \int_0^1 \Big[(C^T I^\beta \Psi^{h,\alpha}_{k,M}(t) + 1)^2 + \left(E^T I^\beta \Psi^{h,\alpha}_{k,M}(t) + 1\right)^2 + \left(C^T \Psi^{h,\alpha}_{k,M}(t) + C^T I^\beta \Psi^{h,\alpha}_{k,M}(t) + 1 - (E^T I^\beta \Psi^{h,\alpha}_{k,M}(t) + 1)\right)^2\Big] dt, \tag{3.32}$$

subject to

$$E^T \Psi^{h,\alpha}_{k,M}(t) = -2\,(E^T I^\beta \Psi^{h,\alpha}_{k,M}(t) + 1). \tag{3.33}$$

The problem in Eqs. (3.32)-(3.33) is a parameter optimization problem. This problem has been solved by applying the Bernoulli wavelet method in [11]. For this example, the authors in [11] give the errors for $x_1(t)$, $x_2(t)$, and $u(t)$ for the case $\beta = 1$. In addition, they draw the graphs of the approximation of $x_1(t)$, $x_2(t)$, and $u(t)$ for the case $0.8 < \beta < 1$. In order to compare our method with the method in [11], we also consider the same values of β. Table 3.7 on page 37 represents a comparison between absolute errors of the cost functional J and L_2 norm errors of control and state functions obtained by our method with $\alpha = \beta = k = 1$, and Bernoulli wavelet method with $\beta = k = 1$, and several values of M and M_4. In addition, the plots of absolute error functions of $x_1(t)$, $x_2(t)$ and $u(t)$ obtained by the proposed method for $k = 1$, and $M = 6$ are represented in figure 3.2 on page 38, and the plots of approximate functions of $x_1(t)$, $x_2(t)$, and $u(t)$ for $k = 1$, $M = 4$ and several values of β along with the exact functions are given in figure 3.3 on page 39. Clearly, the approximate solutions tend to the exact ones given for $\beta = 1$.

Example 3.2.6. We consider the following cancer model [36]:

$$min \quad J(u) = \int_0^1 \left(20\,T(t) - N(t) + u^2(t)\right) dt, \tag{3.34}$$

subject to the nonlinear fractional differential system

$$D^{\beta}T(t) = 1.5\,T(t)\,(1 - T(t)) - 0.5\,T(t)I(t) - T(t)N(t) + 1.5\,T(t)F(t) - 0.08\,D_1(t)T(t), \tag{3.35}$$

$$D^{\beta}I(t) = 0.33 + 0.01\frac{T(t)I(t)}{0.3 + T(t)} - 0.5\,T(t)I(t) - 0.2\,I(t) - 2 \times 10^{-11} D_1(t)I(t), \tag{3.36}$$

$$D^{\beta}N(t) = N(t)\,(1 - N(t)) - T(t)N(t) - 0.008 D_1(t)N(t), \tag{3.37}$$

$$D^{\beta}F(t) = 0.75\,F(t)(1 - 1.5\,F(t)) - 0.1\,T(t)F(t) - 0.008\,D_1(t)F(t), \tag{3.38}$$

$$D^{\beta}D_1(t) = u(t) - 0.1\,D_1(t), \tag{3.39}$$

where $T(t)$ stands for tumor cells, $I(t)$ immune cells, $N(t)$ normal cells, and $F(t)$ fat cells around tumor cells at time t. $D_1(t)$ is the chemotherapeutic drug, and $u(t)$ is the dose of this drug that is injected (for more details about the model, see [36]). The initial conditions are

$$T(0) = 1,\ I(0) = 0.001,\ N(0) = 4,\ F(0) = 0.25,\ D_1(0) = 0.5. \tag{3.40}$$

We solve this problem for $\beta = 0.95$ that is used in [36], $\alpha = 1$, $k = 1$, and $M = 4$. First, we expand $D^{\beta}T(t)$, $D^{\beta}I(t)$, $D^{\beta}N(t)$, $D^{\beta}F(t)$, and $D^{\beta}D_1(t)$ by GFOCW as follows:

$$\begin{aligned}
D^{\beta}T(t) &= C_1^T \Psi_{1,4}^{1,1}(t),\\
D^{\beta}I(t) &= C_2^T \Psi_{1,4}^{1,1}(t),\\
D^{\beta}N(t) &= C_3^T \Psi_{1,4}^{1,1}(t),\\
D^{\beta}F(t) &= C_4^T \Psi_{1,4}^{1,1}(t),\\
D^{\beta}D_1(t) &= C_5^T \Psi_{1,4}^{1,1}(t),
\end{aligned} \tag{3.41}$$

where C_i for $i = 1, ..., 5$ and $\Psi_{1,4}^{1,1}$ are given in Eqs. (2.6) and (2.7). Next, by applying the operator I^β in Eq. (3.41), we get

$$T(t) = C_1^T I^\beta \Psi_{1,4}^{1,1}(t) + 1, \tag{3.42}$$

$$I(t) = C_2^T I^\beta \Psi_{1,4}^{1,1}(t) + 0.001, \tag{3.43}$$

$$N(t) = C_3^T I^\beta \Psi_{1,4}^{1,1}(t) + 4, \tag{3.44}$$

$$F(t) = C_4^T I^\beta \Psi_{1,4}^{1,1}(t) + 0.25, \tag{3.45}$$

$$D_1(t) = C_5^T I^\beta \Psi_{1,4}^{1,1}(t) + 0.5. \tag{3.46}$$

Then, by substituting $D^\beta D_1(t)$ from Eq. (3.41) and $D_1(t)$ from Eq. (3.46) in Eq. (3.39), we obtain

$$u(t) = C_5^T \Psi_{1,4}^{1,1}(t) + 0.1\, C_5^T I^\beta \Psi_{1,4}^{1,1}(t) + 0.05. \tag{3.47}$$

Finally, after substituting Eqs. (3.41)-(3.47) in the performance index J in Eq. (3.34), and in the differential equations in Eqs. (3.35)-(3.39), the problem is reduced to a parameter optimization problem. The approximate functions obtained for the states and control variables are shown in figure 3.4 on page 40. From this figure, we can conclude that over time, the number of tumor cells (T(t)) decreases, the immune and fat cells population increase, while the drug concentration and its dose decline after destroying most of the tumor cells.

3.3 Fractional-order optimal control problems with inequality constraints

In this section, we solve fractional-order optimal control problems (FOCPs) with inequality constraints involving state and control inequality constraints.

3.3.1 Problem statement and numerical method

We study the following FOCP:

$$min \quad J(x,u) = \int_0^1 \mathcal{F}\left(t, x(t), u(t)\right)\, dt, \tag{3.48}$$

subject to the dynamical system

$$D^{\beta}x(t) = \mathcal{G}\left(t, x(t)\right) + \nu(t)u(t), \quad n-1 < \beta \leq n, \text{ for } n \in \mathbb{N}, \tag{3.49}$$

with the inequality constraint

$$\mathcal{H}(t, x(t), u(t)) \leq 0, \tag{3.50}$$

and

$$x^{(k)}(0) = \lambda_k, \quad k = 0, 1, 2, ..., n-1, \tag{3.51}$$

where $\nu(t) \neq 0$, $\mathcal{F}$, $\mathcal{G}$ and $\mathcal{H}$ are continuous functions.

To solve this problem, first we expand $D^{\beta}x(t)$ by using GFOCW as

$$D^{\beta}x(t) \simeq C^T \Psi^{h,\alpha}_{k,M}(t), \tag{3.52}$$

where C, and $\Psi^{h,\alpha}_{k,M}(t)$ are defined in equations (2.6) and (2.7) respectively. Then from equation (3.52), we get

$$x(t) \simeq C^T I^{\beta} \Psi^{h,\alpha}_{k,M}(t) + \sum_{k=0}^{n-1} \frac{\lambda_k}{k!} t^k. \tag{3.53}$$

By using equations (3.49), (3.52), and (3.53), we get

$$u(t) \simeq \frac{C^T \Psi^{h,\alpha}_{k,M}(t) - \mathcal{G}\left(t, C^T I^{\beta} \Psi^{h,\alpha}_{k,M}(t) + \sum\limits_{k=0}^{n-1} \frac{\lambda_k}{k!} t^k\right)}{\nu(t)}. \tag{3.54}$$

By applying equations (3.53) and (3.54) in equation (3.48), we have

$$J = J(x,u) = \int_0^1 \mathcal{F}\left(t, C^T I^{\beta}\Psi_{k,M}^{h,\alpha}(t) + \sum_{k=0}^{n-1}\frac{\lambda_k}{k!}t^k, \frac{C^T\Psi_{k,M}^{h,\alpha}(t) - \mathcal{G}\left(t, C^T I^{\beta}\Psi_{k,M}^{h,\alpha}(t) + \sum_{k=0}^{n-1}\frac{\lambda_k}{k!}t^k\right)}{\nu(t)}\right). \tag{3.55}$$

For the inequality constraints, we substitute equations (3.53) and (3.54) in equation (3.50), and we get

$$\mathcal{H}\left(t, C^T I^{\beta}\Psi_{k,M}^{h,\alpha}(t) + \sum_{k=0}^{n-1}\frac{\lambda_k}{k!}t^k, \frac{C^T\Psi_{k,M}^{h,\alpha}(t) - \mathcal{G}\left(t, C^T I^{\beta}\Psi_{k,M}^{h,\alpha}(t) + \sum_{k=0}^{n-1}\frac{\lambda_k}{k!}t^k\right)}{\nu(t)}\right) \leq 0. \tag{3.56}$$

Now, by collocating equation (3.56) at the following Newton-Cotes nodes given in [109]:

$$t_i = \left(\frac{2i-1}{2^k(M+1)}\right)^{1/\alpha} h, \quad i = 1, ..., 2^{k-1}(M+1), \tag{3.57}$$

we have

$$\mathcal{H}\left(t_i, C^T I^{\beta}\Psi_{k,M}^{h,\alpha}(t_i) + \sum_{k=0}^{n-1}\frac{\lambda_k}{k!}t_i^k, \frac{C^T\Psi_{k,M}^{h,\alpha}(t_i) - \mathcal{G}\left(t_i, C^T I^{\beta}\Psi_{k,M}^{h,\alpha}(t_i) + \sum_{k=0}^{n-1}\frac{\lambda_k}{k!}t_i^k\right)}{\nu(t_i)}\right) \leq 0. \tag{3.58}$$

Next, we minimize J in equation (3.55) subject to equation (3.58) by using known methods. Finally, by obtaining C, the values of $x(t), u(t)$ and the cost functional J can be evaluated.

3.3.2 Illustrative examples

Example 3.3.2.1. We consider the following FOCP [51], [101] ,[105]

$$min \quad J(x,u) = \int_0^1 \left(x^2(t) + u^2(t) - 2(1 - t^{\frac{3}{2}})\, u(t) + 2\, t^{\frac{3}{2}} x(t)\right) dt, \tag{3.59}$$

subject to

$$D^{\frac{3}{2}}x(t) = \frac{3\sqrt{\pi}}{4}(x(t) - u(t)), \tag{3.60}$$

$$x(t) \leq 0, \tag{3.61}$$

$$0 \leq u(t) \leq 1, \tag{3.62}$$

$$x(0) = \dot{x}(0) = 0. \tag{3.63}$$

The optimal solutions are $x(t) = -t^{\frac{3}{2}}$, $u(t) = -t^{\frac{3}{2}} + 1$, with $J = -0.7$.

To solve this problem, we use $\alpha = 1$, $k = 1$, and $M = 2$. First, we expand $D^{\frac{3}{2}}x(t)$ by GFOCW as

$$D^{\frac{3}{2}}x(t) = C^T\Psi^{1,1}_{1,2}(t). \tag{3.64}$$

Then,

$$x(t) = C^T I^{\frac{3}{2}}\Psi^{1,1}_{1,2}(t). \tag{3.65}$$

Now, by using equations (3.64) and (3.65) in equation (3.60), we get

$$u(t) = \frac{-4}{3\sqrt{\pi}}(C^T\Psi^{1,1}_{1,2}(t) - \frac{3\sqrt{\pi}}{4}(C^T I^{\frac{3}{2}}\Psi^{1,1}_{1,2}(t)). \tag{3.66}$$

Next, we use equations (3.65) and (3.66) in equations (3.61) and (3.62) to get

$$C^T I^{\frac{3}{2}}\Psi^{1,1}_{1,2}(t) \leq 0, \tag{3.67}$$

$$0 \leq \frac{-4}{3\sqrt{\pi}}(C^T\Psi^{1,1}_{1,2}(t) - \frac{3\sqrt{\pi}}{4}(C^T I^{\frac{3}{2}}\Psi^{1,1}_{1,2}(t)) \leq 1 \tag{3.68}$$

After that, we collocate the above equations at the nodes defined in equation (3.57). Finally, by substituting equations (3.65) and (3.66) in equation (3.59), and after solving this problem, we

obtain the values for the unknown parameters as $C = [c_{1,0}, c_{1,1}, c_{1,2}]^T = [\frac{-3\pi}{4\sqrt{2}}, 0, 0]^T$ which gives the exact solutions given by

$$x(t) = \frac{-3\pi}{4\sqrt{2}} \sqrt{\frac{2}{\pi}} \left(\frac{4t^{\frac{3}{2}}}{3\sqrt{\pi}} \right) = -t^{\frac{3}{2}}, \quad u(t) = -t^{\frac{3}{2}} + 1, \quad J = -0.7.$$

This problem has been solved in [51] by using epsilon penalty Ritz method, in [101] by applying fractional-order Bernoulli wavelets, and in [105] by Chebyshev wavelet method. Neither of these methods could obtain the exact solution.

Example 3.3.2.2. Consider the following FOCP [101]

$$min \quad J(x,u) = \int_0^1 \left((x(t) - t^2)^2 + (u(t) - t^{\frac{4}{3}})^2 \right) dt, \tag{3.69}$$

subject to

$$D^\beta x(t) = t^{\frac{2}{3}} x(t)u(t) - (t^4 - 2t),$$

$$0 \leq x(t) + u(t) \leq 2,$$

$$x(0) = 0.$$

The exact solution of this problem for $\beta = 1$ is $x(t) = t^2$, $u(t) = t^{\frac{4}{3}}$, and $J = 0$. To solve this problem for $\beta = 1$, we choose $\alpha = \frac{1}{3}$, $k = 1$, and $M = 5$. First, we write $D^\beta x(t)$ and $u(t)$ as

$$D^\beta x(t) = C^T \Psi_{1,5}^{1,\frac{1}{3}}(t), \tag{3.70}$$

$$u(t) = E^T \Psi_{1,5}^{1,\frac{1}{3}}(t). \tag{3.71}$$

Then by applying the RLFIO on $D^\beta x(t)$ in equation (3.70), we get

$$x(t) = C^T I^\beta \Psi_{1,5}^{1,\frac{1}{3}}(t). \tag{3.72}$$

Now, by using the same procedure applied in Example 3.3.2.1, we obtain the following values for the unknowns vectors C, and D

$$C = [\frac{7\sqrt{\pi/2}}{16}, \frac{7\sqrt{\pi}}{32}, \frac{3\sqrt{\pi}}{32}, \frac{\sqrt{\pi}}{64}, 0]^T, \tag{3.73}$$

$$E = [\frac{21\sqrt{\pi/2}}{128}, \frac{3\sqrt{\pi}}{32}, \frac{27\sqrt{\pi}}{512}, \frac{\sqrt{\pi}}{64}, \frac{\sqrt{\pi}}{512}]^T. \tag{3.74}$$

By substituting the above values for C and E, in equations (3.69), (3.71), and (3.72), we obtain the exact solution. This solution was not obtained in [101] by applying fractional Bernoulli wavelets.

Example 3.3.2.3. Consider the following FOCP [61, 68, 107]

$$min \quad J(x,u) = \int_0^1 (-ln\,2)x(t)dt, \tag{3.75}$$

subject to

$$D^\beta x(t) = ln2\,(x(t) + u(t)), \tag{3.76}$$

$$x(t) + u(t) \leq 2, \tag{3.77}$$

$$|u(t)| \leq 1, \tag{3.78}$$

with $x(0) = 0$. When $\beta = 1$, the exact solutions are given in Ref. [68] as $x(t) = 2^t - 1$, $u(t) = 1$ and the optimal cost functional with 9 digits is $J = -0.306852819$. We solve the problem by applying the proposed approach for $\beta = 1$, and several values of α, k and M. First, we write $D^\beta x(t)$ as

$$D^\beta x(t) = C^T \Psi^{1,1}_{k,M}(t). \tag{3.79}$$

Then,

$$x(t) = C^T I^\beta \Psi^{1,1}_{k,M}(t). \tag{3.80}$$

Now, by using equations (3.76), (3.79) and (3.80), we get

$$u(t) = \frac{C^T \Psi^{1,1}_{k,M}(t) - ln2\, C^T I^{\beta} \Psi^{1,1}_{k,M}(t)}{ln2}. \tag{3.81}$$

Next, we substitute $x(t)$ and $u(t)$ from equations (3.80) and (3.81) in the inequality constraints given in equations (3.77) and (3.78) and then collocate at the nodes defined in equation (3.57).

$$C^T I^{\beta} \Psi^{1,1}_{k,M}(t) + \frac{C^T \Psi^{1,1}_{k,M}(t) - ln2\, C^T I^{\beta} \Psi^{1,1}_{k,M}(t)}{ln2} \leq 2,$$
$$-1 \leq \frac{C^T \Psi^{1,1}_{k,M}(t) - ln2\, C^T I^{\beta} \Psi^{1,1}_{k,M}(t)}{ln2} \leq 1.$$

Finally, by substituting $x(t)$ and $u(t)$ in equation (3.75), we obtain a parameter optimization problem. By solving the last problem, we can obtain the values of C.

In Table 3.8 on page 37, we get the AE values for J with $k = 2$ and several values of α and M by using our method. This table suggests that $\alpha = 1$ results in the best AE values for our method. Table 3.9 on page 41 provides a comparison between the evaluated J values obtained for $\beta = 1$ by the proposed method and the methods in [4, 61, 68, 107]. In this table, M_i, $(i = 4, 5, 6, 7)$, are the degrees of the hat functions, Bernoulli, Taylor, and Bernstein polynomials, respectively. In Table 3.10 on page 42, the l_2-norm error values of $x(t)$ and $u(t)$ are compared between the present method and the method in [68]. In this table, $E_M x(t)$ and $E_M u(t)$ are the l_2-norm of the errors of $x(t)$ and $u(t)$ and they are given in [68] by

$$E_M x(t) = \left(\frac{1}{2^{k-1}(M+1)} \sum_{j=1}^{2^{k-1}(M+1)} \left(x(t_j) - x_M(t_j) \right)^2 \right)^{\frac{1}{2}},$$
$$E_M u(t) = \left(\frac{1}{2^{k-1}(M+1)} \sum_{j=1}^{2^{k-1}(M+1)} \left(u(t_j) - u_M(t_j) \right)^2 \right)^{\frac{1}{2}},$$

where $t_j = \frac{j}{2^{k-1}(M+1)}, \quad j = 0, 1, ..., 2^{k-1}(M+1)$.

In addition, the graphs of AE functions of $x(t)$ and $u(t)$ are shown in figure 3.5 on page 42.

Table 3.1

Comparison of absolute errors of $x(t)$ produced by the proposed method and Bessel wavelet approach [26] with $\alpha = 1$ for Example 3.2.2

	Present method ($k = 1$, $M = 5$)			Bessel wavelets ($k = 1$, $M_2 = 5$)		
t	$\beta = 0.8$	$\beta = 0.9$	$\beta = 1$	$\beta = 0.8$	$\beta = 0.9$	$\beta = 1$
0	0	0	0	3.84×10^{-29}	3.42×10^{-29}	2.79×10^{-28}
0.1	6.65×10^{-7}	3.09×10^{-7}	0	1.49×10^{-5}	7.50×10^{-6}	3.30×10^{-16}
0.2	1.09×10^{-6}	4.85×10^{-7}	0	4.23×10^{-6}	2.71×10^{-6}	1.95×10^{-17}
0.3	1.26×10^{-6}	5.34×10^{-7}	0	3.65×10^{-6}	2.21×10^{-6}	3.35×10^{-16}
0.4	1.53×10^{-6}	6.57×10^{-7}	0	9.09×10^{-6}	4.52×10^{-6}	3.52×10^{-16}
0.5	3.01×10^{-7}	1.38×10^{-7}	0	1.10×10^{-5}	5.39×10^{-6}	1.16×10^{-16}
0.6	1.39×10^{-6}	6.23×10^{-7}	0	6.43×10^{-6}	3.30×10^{-6}	1.64×10^{-16}
0.7	1.38×10^{-7}	1.29×10^{-7}	0	1.93×10^{-7}	2.07×10^{-7}	2.63×10^{-16}
0.8	1.30×10^{-6}	5.53×10^{-7}	0	1.44×10^{-6}	5.62×10^{-7}	7.85×10^{-17}
0.9	2.44×10^{-7}	1.10×10^{-7}	0	4.05×10^{-6}	1.75×10^{-6}	2.23×10^{-16}
1	1.87×10^{-17}	5.72×10^{-18}	0	4.37×10^{-17}	2.79×10^{-17}	6.10×10^{-17}

Table 3.2

Comparison of absolute errors of $u(t)$ with $\alpha = 1$ for Example 3.2.2

t	Present method ($k = 1$, $M = 5$)			Bessel wavelets ($k = 1$, $M_2 = 5$)		
	$\beta = 0.8$	$\beta = 0.9$	$\beta = 1$	$\beta = 0.8$	$\beta = 0.9$	$\beta = 1$
0	1.25×10^{-5}	5.11×10^{-5}	0	2.71×10^{-4}	1.29×10^{-4}	2.07×10^{-14}
0.1	5.38×10^{-5}	2.54×10^{-6}	0	1.09×10^{-4}	5.58×10^{-5}	3.14×10^{-15}
0.2	2.69×10^{-6}	1.37×10^{-6}	0	5.49×10^{-5}	2.79×10^{-5}	8.18×10^{-15}
0.3	3.18×10^{-5}	1.49×10^{-5}	0	6.20×10^{-5}	2.93×10^{-5}	3.93×10^{-15}
0.4	1.31×10^{-6}	7.13×10^{-6}	0	8.01×10^{-5}	3.73×10^{-5}	2.34×10^{-15}
0.5	3.19×10^{-7}	1.55×10^{-6}	0	8.41×10^{-7}	3.09×10^{-6}	5.93×10^{-15}
0.6	4.22×10^{-7}	1.48×10^{-7}	0	9.41×10^{-7}	4.71×10^{-5}	4.75×10^{-15}
0.7	2.89×10^{-5}	1.43×10^{-7}	0	9.05×10^{-5}	4.59×10^{-5}	4.33×10^{-16}
0.8	1.33×10^{-6}	6.07×10^{-6}	0	8.97×10^{-5}	9.85×10^{-6}	5.81×10^{-15}
0.9	1.45×10^{-5}	1.69×10^{-7}	0	2.21×10^{-5}	4.54×10^{-5}	4.40×10^{-15}
1	2.23×10^{-5}	3.46×10^{-5}	0	2.87×10^{-4}	1.44×10^{-4}	1.41×10^{-14}

Table 3.3

Comparison between approximate values of J for various values of β and $\alpha = 1$, for Example 3.2.2

	$\beta = 0.7$	$\beta = 0.8$	$\beta = 0.85$	$\beta = 0.9$	$\beta = 1$
Present method ($k = 1$, $M = 5$)	2.4377×10^{-9}	1.0298×10^{-9}	5.6172×10^{-10}	2.4152×10^{-10}	0
Bessel method ($k = 1$, $M_2 = 5$)	1.5115×10^{-8}	7.0650×10^{-9}	—	1.7599×10^{-9}	0

Table 3.4

Comparison between absolute error values of functions J, x(t), and u(t), at $\beta = 1$ with $\alpha = 0.5$, for Example 3.2.3

t	Present method ($k = 1$, $M = 2$)			Bessel wavelet ($k = 1$, $M_2 = 5$) [26]		
	$e_{x(t)}$	$e_{u(t)}$	e_J	$e_{x(t)}$	$e_{u(t)}$	e_J
0	0	5.5511×10^{-17}	4.6906×10^{-33}	1.7698×10^{-25}	9.3526×10^{-2}	—
0.1	6.9389×10^{-18}	5.5511×10^{-17}		3.8755×10^{-2}	4.4211×10^{-3}	
0.2	9.5409×10^{-18}	0		4.4015×10^{-2}	9.8306×10^{-3}	
0.3	1.0408×10^{-17}	8.3267×10^{-17}		3.9146×10^{-2}	1.1924×10^{-2}	
0.4	0	2.7755×10^{-17}		2.8318×10^{-2}	1.0805×10^{-2}	
0.5	0	6.9389×10^{-17}		1.4636×10^{-2}	1.0656×10^{-2}	
0.6	0	0		8.0523×10^{-4}	1.2465×10^{-5}	
0.7	3.8164×10^{-17}	4.1633×10^{-17}		1.0706×10^{-2}	1.5475×10^{-2}	
0.8	7.9797×10^{-17}	4.1633×10^{-17}		1.7596×10^{-2}	1.8067×10^{-2}	
0.9	1.3878×10^{-17}	4.1633×10^{-17}		1.7695×10^{-2}	1.8344×10^{-2}	
1	8.3267×10^{-17}	3.0646×10^{-17}		8.9399×10^{-2}	1.4570×10^{-2}	

Table 3.5

Comparison between error values of J at $\beta = 1$ for Example 3.2.4

Method	e_J
Proposed method	
$(k = 2, M = 3)$	1.35602×10^{-8}
$(k = 2, M = 4)$	1.67671×10^{-9}
$(k = 2, M = 5)$	5.32699×10^{-10}
$(k = 2, M = 6)$	2.57362×10^{-10}
Bernoulli wavelets [11]	
$(k = 2, M_4 = 4)$	3.45331×10^{-7}
$(k = 2, M_4 = 5)$	1.19358×10^{-7}
$(k = 2, M_4 = 6)$	4.21388×10^{-8}
$(k = 2, M_4 = 7)$	1.75609×10^{-8}

Table 3.6

Comparison between L_2 errors of the functions x(t) and u(t), for Example 3.2.4

Method	L_2 error of x(t)	L_2 error of u(t)
Proposed method		
$(k = 2, M = 2)$	6.13213×10^{-6}	2.17741×10^{-4}
$(k = 2, M = 4)$	1.27887×10^{-7}	5.89366×10^{-5}
$(k = 2, M = 6)$	1.73215×10^{-7}	1.87711×10^{-5}
Bernoulli wavelets		
$(k = 2, M_4 = 3)$	6.46147×10^{-5}	5.04006×10^{-3}
$(k = 2, M_4 = 5)$	7.34298×10^{-6}	4.88532×10^{-4}
$(k = 2, M_4 = 7)$	1.76367×10^{-6}	1.87480×10^{-4}

Table 3.7

The absolute error values of J and L_2 norm errors of control and state functions at $\beta = 1$ for Example 3.2.5

	e_J	L_2 error of $x_1(t)$	L_2 error of $x_2(t)$	L_2 error of $u(t)$
Proposed method				
$k = 2, M = 4$	4.09635×10^{-6}	4.74779×10^{-6}	6.91619×10^{-7}	1.04247×10^{-6}
$k = 2, M = 5$	3.72269×10^{-6}	4.58891×10^{-6}	6.41141×10^{-8}	5.45539×10^{-7}
$k = 2, M = 6$	3.68642×10^{-6}	4.57692×10^{-6}	1.55831×10^{-9}	5.26672×10^{-7}
$k = 1, M = 4$	2.43644×10^{-5}	2.18562×10^{-5}	2.95435×10^{-5}	1.64708×10^{-6}
$k = 1, M = 5$	5.76070×10^{-6}	5.53117×10^{-6}	2.89979×10^{-6}	2.48669×10^{-6}
$k = 1, M = 6$	3.87449×10^{-6}	4.64578×10^{-6}	2.59723×10^{-7}	2.33632×10^{-6}
Bernoulli wavelet method				
$k = 1, M_4 = 5$	—	1.16095×10^{-4}	1.22992×10^{-4}	2.73136×10^{-5}
$k = 1, M_4 = 6$	—	1.19411×10^{-5}	1.02083×10^{-5}	3.92688×10^{-6}
$k = 1, M_4 = 7$	—	4.66170×10^{-6}	7.27096×10^{-7}	1.39120×10^{-6}

Table 3.8

The AE values of J obtained by our method at $\beta = 1$ with different α for Example 3.3.2.3

(k, M)	$\alpha = 0.25$	$\alpha = 0.5$	$\alpha = 0.75$	$\alpha = 1$	$\alpha = 1.5$	$\alpha = 2$
$k = 2, M = 2$	2.81×10^{-1}	1.59×10^{-1}	1.33×10^{-1}	$\mathbf{1.09 \times 10^{-5}}$	2.69×10^{-2}	1.90×10^{-1}
$k = 2, M = 3$	2.74×10^{-1}	1.93×10^{-1}	1.33×10^{-1}	$\mathbf{4.18 \times 10^{-7}}$	2.69×10^{-2}	3.34×10^{-1}
$k = 2, M = 4$	2.84×10^{-1}	1.63×10^{-1}	1.33×10^{-1}	$\mathbf{5.35 \times 10^{-9}}$	1.72×10^{-1}	5.41×10^{-1}
$k = 2, M = 5$	2.64×10^{-1}	1.93×10^{-1}	1.33×10^{-1}	$\mathbf{6.74 \times 10^{-10}}$	3.37×10^{-1}	7.19×10^{-1}

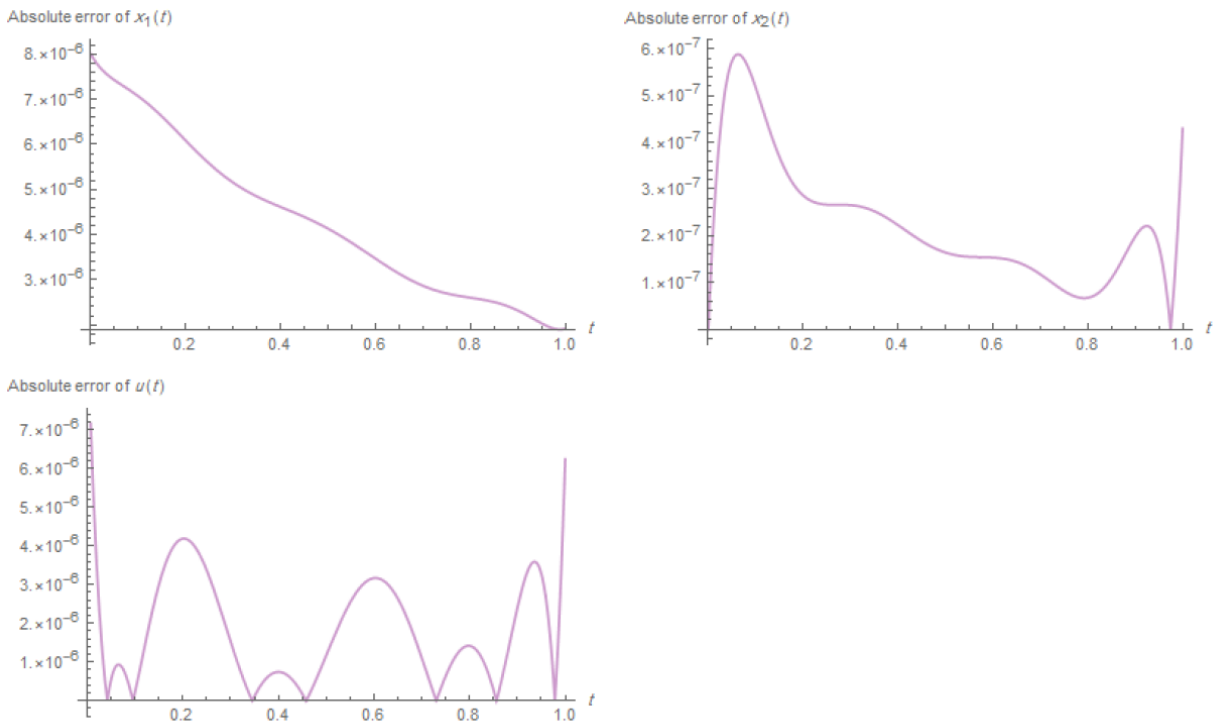

Figure 3.2

Graphs of absolute error functions of $x_1(t)$, $x_2(t)$, and $u(t)$ for $\alpha = \beta = 1$, $k = 1$, and $M = 6$ for Example 3.2.5

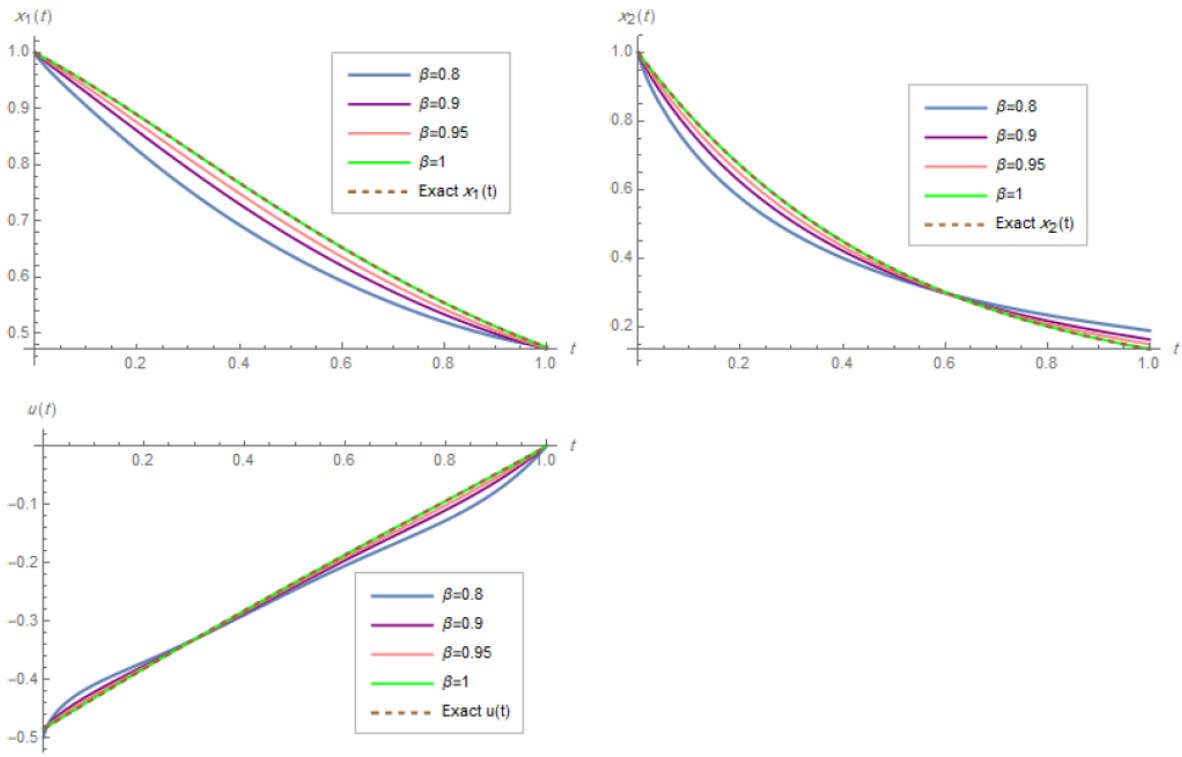

Figure 3.3

Graphs of the approximate functions of $x_1(t)$, $x_2(t)$, and $u(t)$ for $k = 1$, $M = 4$, and several values of β along with the exact functions for Example 3.2.5

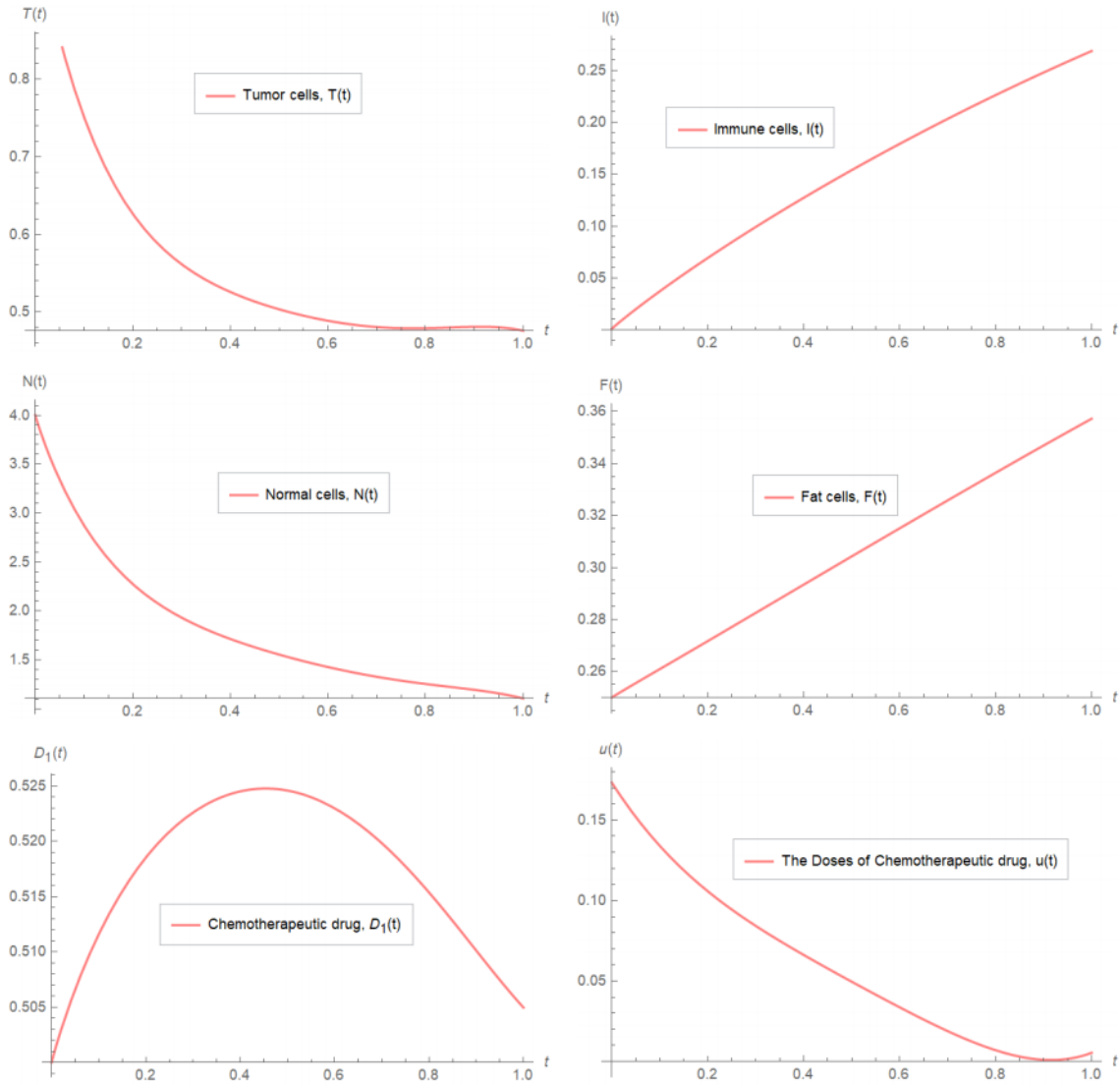

Figure 3.4

Numerical values of $T(t)$, $I(t)$, $N(t)$, $F(t)$, $D_1(t)$, and $u(t)$ for Example 3.2.6

Table 3.9

A comparison of the evaluated values of J, between different methods for Example 3.3.2.3

Method	J	e_J
Bernstein polynomials 2013 [4]		
$M_2 = 3$	-0.30685	2.82×10^{-6}
Bernoulli hybrid functions 2018 [61]		
$N = 1, M_5 = 3$	-0.30683	2.28×10^{-5}
Taylor hybrid functions 2018 [107]		
$N = 1, M_6 = 3$	-0.30683	2.29×10^{-5}
Modified hat functions 2019 [68]		
$M_7 = 8$	-0.3068511	1.72×10^{-6}
$M_7 = 16$	-0.3068527	1.19×10^{-7}
$M_7 = 32$	-0.3068528	1.94×10^{-8}
Present method		
$k = 1, M = 3$	-0.306854727	8.09×10^{-6}
$k = 1, M = 5$	-0.306853257	4.38×10^{-7}
$k = 2, M = 3$	-0.306852901	4.18×10^{-7}
$k = 2, M = 5$	-0.306852820	6.74×10^{-10}
$k = 3, M = 3$	-0.306852794	2.45×10^{-8}
$k = 3, M = 4$	-0.3068528195	8.32×10^{-11}
J given in [68]	-0.306852819	

Table 3.10

The l_2-norm errors of the state and control variables for Example 3.3.2.3

Method	$E_M x(t)$	$E_M u(t)$
Proposed method		
$k = 1, M = 3$	1.6951×10^{-5}	2.8690×10^{-4}
$k = 1, M = 5$	8.4380×10^{-6}	3.1356×10^{-4}
$k = 2, M = 3$	8.0694×10^{-7}	1.3211×10^{-5}
$k = 2, M = 5$	7.3816×10^{-9}	2.8974×10^{-7}
Modified hat functions 2019 [68]		
$M_7 = 2$	8.07×10^{-4}	—
$M_7 = 4$	4.99×10^{-5}	—
$M_7 = 8$	3.09×10^{-6}	—
$M_7 = 16$	1.92×10^{-7}	—
$M_7 = 32$	1.20×10^{-8}	—

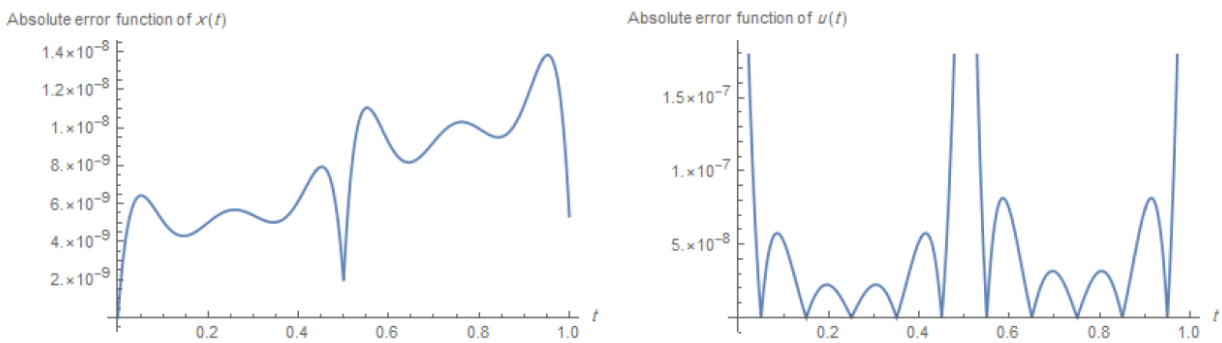

Figure 3.5

The AE functions of $x(t)$ and $u(t)$ for $\alpha = \beta = 1$, $k = 2$ and $M = 4$ for Example 3.3.2.3

CHAPTER IV

DISTRIBUTED-ORDER FRACTIONAL OPTIMAL CONTROL PROBLEMS

The fractional differential operators in dynamical systems not only appear as discrete fractional, but they also possess a continuous nature in a sense that their order is distributed over a given range [110]. Distributed-order fractional models have pore flexibility to explain real physical phenomena in disordered, viscoelastic media, and composite materials [19, 48, 62, 95, 92].

This section focuses on solving optimal control problems containing distributed-order fractional derivatives.

Definition 3

For $\rho(\mu) \geq 0$, $\rho(\mu) \neq 0$, $\int_0^1 \rho(\mu)d\mu < \infty$, *and* $\mu \in (0,1)$, *the distributed-order of* $f(x)$ *is given by*

$$D^{\rho(\mu)} f(x) = \int_0^1 \rho(\mu) D^{\mu} f(x) d\mu. \tag{4.1}$$

4.1 Problem statement and numerical approach

Consider the DO-FOCP

$$min \quad J(x,u) = \int_0^1 F\left(t, x(t), u(t)\right)\, dt, \tag{4.2}$$

subject to

$$D^{\rho(\mu)} x(t) = G\left(t, x(t)\right) + \nu(t)u(t), \quad \mu \in (0,1), \tag{4.3}$$

where

$$D^{\rho(\mu)}x(t) = \int_0^1 \rho(\mu) D^{\mu}x(t)d\mu$$

and

$$x(0) = x_0, \tag{4.4}$$

where $\nu(t) \neq 0$, F, and G are continuous functions.

Remark 1. For the case when $\rho(\mu) = \delta(\mu - \hat{\mu})$, where $\hat{\mu} \in (0, 1)$, the left hand side of Eq. (4.3) becomes $D^{\hat{\mu}}x(t)$ (see [110]).

To solve the problem in Eqs. (4.2)-(4.4), first, by using Eqs. (2.6) and (2.7), we expand $\dot{x}(t)$ by GFOCWs as follows:

$$\dot{x}(t) \simeq C^T \Psi^{h,\alpha}_{k,M}(t). \tag{4.5}$$

Then by applying the operator I^1 in Eq. (4.5), we get

$$x(t) \simeq C^T I^1 \Psi^{h,\alpha}_{k,M}(t) + x_0, \tag{4.6}$$

from the above equation, we can get

$$D^{\mu}x(t) \simeq C^T I^{1-\mu} \Psi^{h,\alpha}_{k,M}(t). \tag{4.7}$$

Then by using Eqs. (4.3), (4.6) and (4.7), we have

$$u(t) \simeq \frac{1}{\nu(t)} \left(\int_0^1 \rho(\mu)(C^T I^{1-\mu} \Psi^{h,\alpha}_{k,M}(t))d\mu - G\left(t, C^T I^1 \Psi^{h,\alpha}_{k,M}(t) + x_0\right)\right). \tag{4.8}$$

Now, by substituting Eqs. (4.6) and (4.8) in the cost function given in (4.2), we get

$$J(x, u) = \int_0^1 F\left(t, C^T I^1 \Psi^{h,\alpha}_{k,M}(t) + x_0, \right. \tag{4.9}$$

$$\left. \frac{1}{\nu(t)} \left(\int_0^1 \rho(\mu)(C^T I^{1-\mu} \Psi^{h,\alpha}_{k,M}(t))d\mu - G\left(t, C^T I^1 \Psi^{h,\alpha}_{k,M}(t) + x_0\right)\right)\right) dt, \tag{4.10}$$

which is a parameter optimization problem that can be solved numerically. Our goal is to find C which minimizes J in Eq. (4.9).

4.2 Error bound for distributed-order fractional derivative

In the following theorems, the error bounds of distributed-order fractional derivative and proposed method are provided.

Theorem 5

Suppose $f \in H^{\xi}(0,1)$ *with* $\xi \geq 0$, $M \geq r$, *and* $\|\rho(\mu)\|_{L^2(0,1)} \leq \mathcal{D}$, *then* [79]

$$\|D^{\rho(\mu)} f - D^{\rho(\mu)}(P_M^{2^{k-1}} f)\|_{L^2(0,1)} \leq 1.085\, \mathcal{D} c M^{2r-\frac{1}{2}-\xi} (2^{k-1})^{r-\xi} \|f^{(\xi)}\|_{L^2(0,1)}. \tag{4.11}$$

Proof: By using Eq. (2.12) given in Theorem 2, we have

$$\begin{aligned}
\|D^{\rho(\mu)} f - D^{\rho(\mu)}(P_M^{2^{k-1}} f)\|_{L^2(0,1)} &= \| \int_0^1 \rho(\mu)(D^{\mu} f - D^{\mu}(P_M^{2^{k-1}} f)\, d\mu \|_{L^2(0,1)} \\
&\leq \int_0^1 \|\rho(\mu)\|_{L^2(0,1)} \|D^{\mu} f - D^{\mu}(P_{M-1}^{2^{k-1}} f\|_{L^2(0,1)}\, d\mu \\
&\leq \int_0^1 \mathcal{D} \frac{c M^{2r-\frac{1}{2}-\xi} (2^{k-1})^{r-\xi} \|f^{(\xi)}\|_{L^2(0,1)}}{\Gamma(2-\mu)}\, d\mu \\
&= 1.085\, \mathcal{D} c M^{2r-\frac{1}{2}-\xi} (2^{k-1})^{r-\xi} \|f^{(\xi)}\|_{L^2(0,1)}.
\end{aligned} \tag{4.12}$$

Thus, the proof is complete. ∎

Theorem 6

Suppose $x(t) \in H^{\xi}(0,1)$ *with* $\xi \geq 0$, $M \geq r$, F *and* G *in the Eqs.* (4.2) *and* (4.3) *is Lipschitz with the Lipschitz constants* λ_1, *and* λ_2 *respectively, and* $\|\frac{1}{\nu(t)}\|_{L^2(0,1)} \leq C$, *then the error bound of the proposed approach is as follows* [79]:

$$\|\mathcal{E}_M^{2^{k-1}}\|_{L^2(0,1)} \leq (\lambda_1 + C\lambda_1\lambda_2)\, cM^{-\xi}(2^{k-1})^{-\xi}\|x^{(\xi)}\|_{L^2(0,1)} + 1.085\, C\lambda_1\, \mathcal{D}cM^{2r-\frac{1}{2}-\xi}(2^{k-1})^{r-\xi}\|x^{(\xi)}\|_{L^2(0,1)}.$$

Proof: According to the problem stated in Eqs. (4.2)-(4.4), we have

$$\begin{aligned}
\left\|\mathcal{E}_M^{2^{k-1}}\right\|_{L^2(0,1)} &= \left\|J(x,u) - J(P_M^{2^{k-1}}x, P_M^{2^{k-1}}u)\right\|_{L^2(0,1)} \\
&= \left\| \int_0^1 F\left(t, x(t), \frac{1}{\nu(t)}\left(D^{\rho(\mu)}x(t) - G(t,x(t))\right)\right)\right. \\
&\quad \left. -F\left(t, P_M^{2^{k-1}}x(t), \frac{1}{\nu(t)}\left(D^{\rho(\mu)}P_M^{2^{k-1}}x(t) - G(t, P_M^{2^{k-1}}x(t))\right)\right)\right\|_{L^2(0,1)} \\
&\leq \lambda_1 \left\|x(t) - P_M^{2^{k-1}}x(t)\right\|_{L^2(0,1)} + C\lambda_1 \left\|D^{\rho(\mu)}x(t) - D^{\rho(\mu)}P_M^{2^{k-1}}x(t)\right\|_{L^2(0,1)} \\
&\quad + C\lambda_1\lambda_2 \left\|x(t) - P_M^{2^{k-1}}x(t)\right\|_{L^2(0,1)} \\
&\leq (\lambda_1 + C\lambda_1\lambda_2)cM^{-\xi}(2^{k-1})^{-\xi}\left\|x^{\xi}\right\|_{L^2(0,1)} \\
&\quad + 1.085\, C\lambda_1\mathcal{D}cM^{2r-\frac{1}{2}-\xi}(2^{k-1})^{r-\xi}\left\|x^{\xi}\right\|_{L^2(0,1)}.
\end{aligned}$$

■

4.3 Illustrative Examples

Example 4.3.1. Consider the DO-FOCP [79, 90]:

$$min \quad J(x,u) = \frac{1}{2}\int_0^1 \left[\left(x(t) - t^{\beta}\right)^2 + \left(u(t) - t^{\beta} - \Gamma(\beta+1)\right)^2\right] dt, \tag{4.13}$$

with

$$\int_0^1 \rho(\mu) D^{\mu} x(t) d\mu = -x(t) + u(t), \quad t \in [0,1] \text{ and } x(0) = 1. \tag{4.14}$$

In the case when $\rho(\mu) = \delta(\mu - \beta)$, the optimal state and control functions are $x(t) = t^{\beta}$, and $u(t) = t^{\beta} + \Gamma(\beta + 1)$, with corresponding minimum cost functional $J_{opt} = 0$. For solving this problem, the authors in [90] have compared the results obtained by Chebyshev wavelet method (CWM), cosine and sine wavelet method (CASWM), Laguerre wavelet method (LaWM), Legendre wavelet method (LWM), and variational iteration method (VIM). Moreover, this problem has been solved in [79] by applying Bernstein wavelet method (BWM) and using the following distribution functions:

$$\begin{cases} \text{Case 1: } \rho(\mu) = \delta(\mu - 1), \\ \text{Case 2: } \rho(\mu) = \delta(\mu - 0.99), \\ \text{Case 3: } \rho(\mu) = \delta(\mu - 0.9), \\ \text{Case 4: } \rho(\mu) = \delta(\mu - 0.8), \\ \text{Case 5: } \rho(\mu) = N^{(0.8,0.05)}(\mu), \\ \text{Case 6: } \rho(\mu) = N^{(0.5,0.1)}(\mu), \end{cases} \tag{4.15}$$

For this problem, by using the distribution functions $\rho(\mu) = \delta(\mu - \beta)$ when $\beta = 1$ and 0.5, we can obtain the exact solutions by selecting $\alpha = \beta$, $k = 1$, and $M = 3$ as follows:

For Case 1, when $\rho(\mu) = \delta(\mu - 1)$, we expand $D^1 x(t)$ by GFOCW as

$$D^1 x(t) = C^T \Psi_{1,3}^{1,1}(t). \tag{4.16}$$

Then,

$$x(t) = C^T I^1 \Psi_{1,3}^{1,1}(t). \tag{4.17}$$

Now, by using Eqs. (4.14)-(4.17), we obtain

$$\begin{aligned} u(t) &= \int_0^1 \delta(\mu - 1) D^\mu x(t) d\mu + x(t) \\ &= C^T \Psi_{1,3}^{1,1}(t) + C^T I^1 \Psi_{1,3}^{1,1}(t). \end{aligned} \tag{4.18}$$

By substituting Eqs. (4.17) and (4.18) in Eq. (4.13), and then finding the minimum of the resulted J, we obtain

$$C = \left[c_{1,0}, c_{1,1}, c_{1,2}\right]^T = \left[\sqrt{\frac{\pi}{2}}, 0, 0\right]^T.$$

Finally we get $x(t) = t, u(t) = 1 + t$, and $J = 0$ which are the exact solutions.

For $\beta = 0.5$, by using the similar argument we get $C = \left[\frac{\pi}{2\sqrt{2}}, 0, 0\right]^T$. For this case, we obtain $x(t) = t^{\frac{1}{2}}$ and $u(t) = t^{\frac{1}{2}} + \frac{1}{2}\sqrt{\pi}$ which are the exact solutions. The exact solutions for the previous case and this case were not obtained in [79] and [90].

For Cases 2-6, our results are compared with those of the BWM given in [79] in Table 4.1 on the next page, Table 4.2 on page 50, and Table 4.3 on page 51. In Table 4.1 on the following page, we compare the absolute errors (AEs) of J by applying our method with $\alpha = 1, k = 2, M = 3$, and the method in [79] with $k = 2, M_1 = 4$ for $\rho(\mu) = \delta(\mu - \beta)$ with $\beta = 0.99, 0.9$, and 0.8. In this table, M_1 is the degree of the Bernstein polynomials. In Table 4.2 on page 50, we compare the AEs of $x(t)$ and $u(t)$ for $\rho(\mu) = \delta(\mu - 0.99)$ by applying our method with $k = 1, M = 4$, and the BWM with $k = 1$ and $M_1 = 10$. In Table 4.3 on page 51, we give the AE values of J with $k = 2, M = 4$ for the present method by using $\rho(\mu) = N^{(0.8,0.05)}(\mu)$ and $N^{(0.5,0.1)}(\mu)$ with several values of α. It is seen from this table that $\alpha = 0.15$ gives the best AE values for J by using the

Table 4.1

Comparison between the AEs of J for different distribution functions for Example 4.3.1

	Present method	BWM [79]
$\rho(\mu)$	$k = 2, M = 3$	$k = 2, M_1 = 4$
$\delta(\mu - 0.99)$	2.5091×10^{-17}	2.11834×10^{-8}
$\delta(\mu - 0.9)$	1.6823×10^{-17}	4.48006×10^{-6}
$\delta(\mu - 0.8)$	2.2767×10^{-17}	4.08630×10^{-5}

present method. We also give the AE values for J obtained by the BWM with $k = 2, M_1 = 4$ and the same distribution $\rho(\mu)$ in this table. Besides, figure 4.1 on page 52 is the graphs of the approximations of $x(t)$ and $u(t)$ by using our method with $\rho(\mu) = N^{(0.8,0.05)}(\mu)$, $\delta(\mu - \beta)$ with $\beta = 1,\ 0.99,\ 0.9$ and 0.8. Figure 4.2 on page 53 is the graphs of the AE functions for $x(t)$ and $u(t)$ by using the present method with $k = 2, M = 4$ and $\rho(\mu) = \delta(\mu - 0.99)$.

Example 4.3.2. Consider the DO-FOCP [79, 90, 110]

$$min \quad J(x,u) = \frac{1}{2}\int_0^1 [x^2(t) + u^2(t)]dt, \tag{4.19}$$

with the dynamical system

$$\int_0^1 \rho(\mu) D^{\mu} x(t) d\mu = u(t) - x(t), \quad t \in [0,1], \text{ and } x(0) = 1. \tag{4.20}$$

For $\rho(\mu) = \delta(\mu - 1)$, the optimal values are

$$x(t) = \eta sinh(\sqrt{2}\,t) + cosh(\sqrt{2}\,t),$$

$$u(t) = (\eta + \sqrt{2})sinh(\sqrt{2}\,t) + (\sqrt{2}\,\eta + 1)cosh(\sqrt{2}\,t),$$

Table 4.2

Comparison of AE values of $x(t)$ and $u(t)$ at $\rho(\mu) = \delta(\mu - 0.99)$ for Example 4.3.1

	Present method ($k = 1, M = 4$)		BWM ($k = 1, M = 10$)	
t	$e_{x(t)}$	$e_{u(t)}$	$e_{x(t)}$	$e_{u(t)}$
0.1	1.68×10^{-17}	8.33×10^{-17}	2.68×10^{-5}	2.68×10^{-5}
0.2	3.20×10^{-17}	2.77×10^{-17}	3.64×10^{-6}	3.64×10^{-6}
0.3	1.21×10^{-17}	1.11×10^{-16}	2.94×10^{-6}	2.94×10^{-6}
0.4	5.56×10^{-18}	5.55×10^{-17}	2.49×10^{-5}	2.49×10^{-5}
0.5	5.08×10^{-17}	2.22×10^{-16}	1.55×10^{-6}	1.55×10^{-6}
0.6	6.45×10^{-17}	2.22×10^{-16}	5.04×10^{-7}	5.04×10^{-7}
0.7	7.34×10^{-17}	3.33×10^{-16}	1.81×10^{-5}	1.81×10^{-5}
0.8	2.59×10^{-17}	1.11×10^{-16}	2.95×10^{-6}	2.95×10^{-6}
0.9	1.38×10^{-17}	3.33×10^{-16}	9.25×10^{-6}	9.25×10^{-6}

where

$$\eta = -\frac{cosh(\sqrt{2}) + \sqrt{2}sinh(\sqrt{2})}{\sqrt{2}cosh(\sqrt{2}) + sinh(\sqrt{2})} \simeq -0.98, \tag{4.21}$$

and

$$J = 0.1929092980931.$$

We solve this problem with the distribution functions as Example 4.3.1 given in Eq. (4.15). Table 4.4 on page 54 and Table 4.5 on page 54 give the AE values for J and the maximal AE values for $x(t)$ and $u(t)$ by using the present method for Cases 1 and 4 in Eq. (4.15), respectively. In these tables, we use $k = 1, M = 4$ and different values of α. Table 4.4 on page 54 and Table 4.5 on page 54 suggest that we get the best results when $\alpha = \beta$. In Table 4.6 on page 55, we compare

Table 4.3

AE values for J for Example 4.3.1

	Present method				BWM
$\rho(\mu)$	$\alpha = \mathbf{0.15}$	$\alpha = 0.5$	$\alpha = 1$	$\alpha = 1.5$	
$N^{(0.8,0.05)}(\mu)$	$\mathbf{1.67 \times 10^{-7}}$	3.77×10^{-6}	2.52×10^{-4}	8.85×10^{-4}	9.69301×10^{-4}
$N^{(0.5,0.1)}(\mu)$	$\mathbf{5.73 \times 10^{-6}}$	1.45×10^{-4}	2.257×10^{-3}	5.69×10^{-3}	9.20957×10^{-3}

the values of J with different distribution functions given in Cases 1-6 in Eq. (4.15) by using our method together with Legendre collocation method (LCM) [110], BWM [79], CWM, LaWM, CASWM, LWM [90], Adomian decomposition method (ADM) [111], and VIM [5].

Example 4.3.3. Consider the following DO-FOCP [79, 90, 110]

$$min \quad J(x,u) = \frac{1}{2}\int_0^1 [x^2(t) + u^2(t)]\,dt, \tag{4.22}$$

subject to

$$\int_0^1 \rho(\mu) D^{\mu} x(t) d\mu = u(t) + t\,x(t), \quad t \in [0,1], \text{ and } x(0) = 1. \tag{4.23}$$

The exact value of J is not known. We solve this problem with $\alpha = 1$ by using $k = 1, 2$ and $M = 4, 5, 6$ for the distribution functions given in Eq. (4.15). Table 4.7 on page 56 gives the values of J by using our method together with Legendre collocation method (LCM) [110], BWM [79], CWM, LaWM, CASWM, LWM [90] and VIM [5]. Figure 4.3 on page 54 gives the graphs of the approximate values of $x(t)$ and $u(t)$ by using our method with $\rho(\mu)$ given in Cases 1-5 in Eq. (4.15).

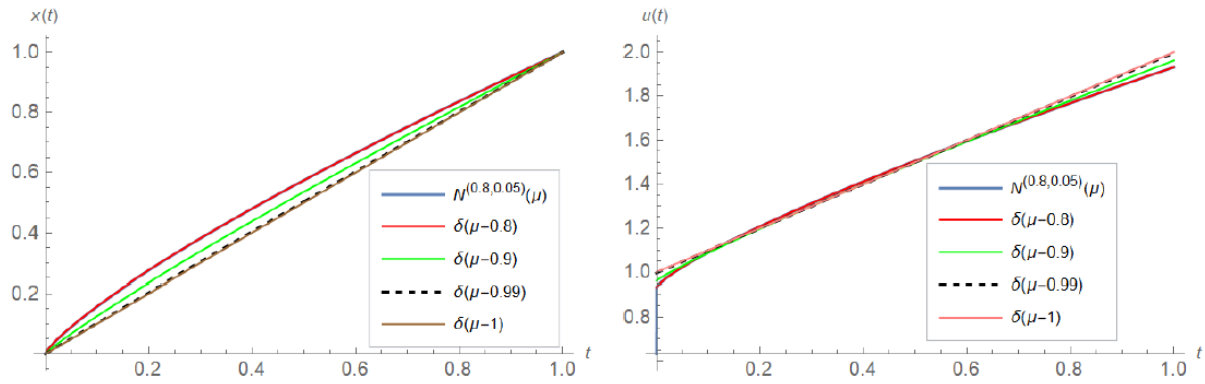

Figure 4.1

The approximate functions of $x(t)$ and $u(t)$ for several distribution functions for Example 4.3.1

Example 4.3.4. Consider the following DO-FOCP [79]

$$min \quad J(x,u) = \frac{1}{2}\int_0^1 \left(0.625\,x^2(t) + 0.5\,x(t)u(t) + 0.5u^2(t)\right), \tag{4.24}$$

subject to

$$\int_0^1 \rho(\mu)D^{\mu}x(t)d\mu = 0.5x(t) + u(t), \quad t \in [0,1], \text{ and } x(0) = 1. \tag{4.25}$$

For $\rho(\mu) = \delta(\mu - 1)$, we have [79]

$$x(t) = \frac{cosh(1-t)}{cosh(1)}, \; u(t) = \frac{-(tanh(1-t) + 0.5)cosh(1-t)}{cosh(1)},$$

and

$$J = \frac{e^2 sinh(2)}{(1+e^2)^2} \simeq 0.38079707797788.$$

The proposed method with $\alpha = 1$ is used to solve this problem for $k = 1, 2$ and $M = 4, 5, 6$. Table 4.8 on page 57 gives the values of J by applying the present method together with the BWM [79] for the distribution functions given in Eq. (4.15). In Table 4.9 on page 58, we give the AE

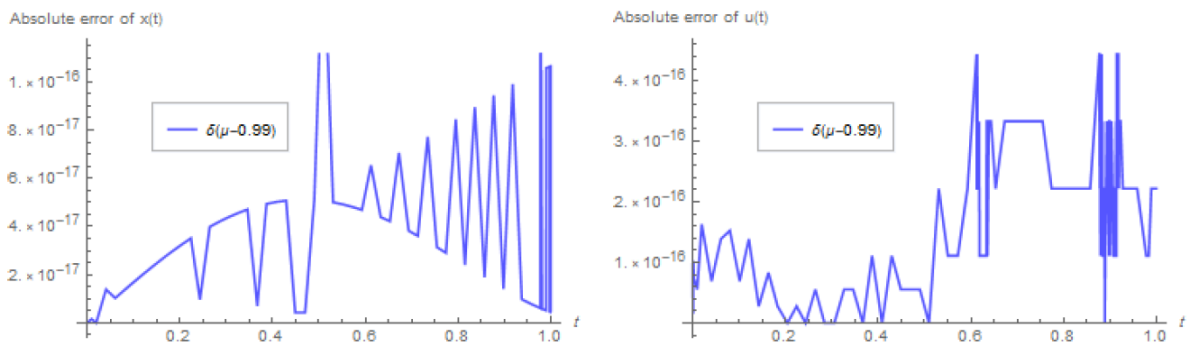

Figure 4.2

The AE functions of $x(t)$ and $u(t)$ with $k = 2, M = 4$ for $\rho(\mu) = \delta(\mu - 0.99)$ for Example 4.3.1

values of $x(t)$ and $u(t)$ when $\rho(\mu) = \delta(\mu - 1)$ by using the present method with $k = 1$, $M = 10$ and the BWM in [79] with $k = 1$ and $M_1 = 10$. Figure 4.4 on page 57 gives the graphs of the approximate values of $x(t)$ and $u(t)$ by applying our method with $k = 2, M = 4$ for the distribution functions given in Eq. (4.15). Figure 4.5 on page 58 shows the AE functions for $x(t)$ and $u(t)$ for the distribution function $\rho(\mu) = \delta(\mu - 1)$.

Table 4.4

AE values for $\rho(\mu) = \delta(\mu - 1)$ with different values of α, $k = 1$ and $M = 4$, for Example 4.3.2

α	0.5	0.75	**1**	1.5	2
e_J	1.15×10^{-6}	7.44×10^{-6}	$\mathbf{1.46 \times 10^{-7}}$	2.03×10^{-4}	9.86×10^{-4}
Max $AE_{x(t)}$	1.97×10^{-4}	4.37×10^{-4}	$\mathbf{6.43 \times 10^{-5}}$	3.17×10^{-3}	8.53×10^{-3}
Max $AE_{u(t)}$	2.02×10^{-3}	6.19×10^{-3}	$\mathbf{1.77 \times 10^{-3}}$	9.11×10^{-2}	1.68×10^{-1}

Table 4.5

AE values for $\rho(\mu) = \delta(\mu - 0.8)$ with different values of α, $k = 1$ and $M = 4$, for Example 4.3.2

α	0.5	0.7	**0.8**	0.9	1
e_J	2.55×10^{-2}	2.58×10^{-2}	$\mathbf{2.51 \times 10^{-2}}$	2.58×10^{-2}	2.58×10^{-2}
Max $e_{x(t)}$	2.76×10^{-2}	2.79×10^{-2}	$\mathbf{2.75 \times 10^{-2}}$	2.82×10^{-2}	2.84×10^{-2}
Max $e_{u(t)}$	1.67×10^{-2}	1.35×10^{-2}	$\mathbf{9.31 \times 10^{-3}}$	2.55×10^{-2}	5.21×10^{-2}

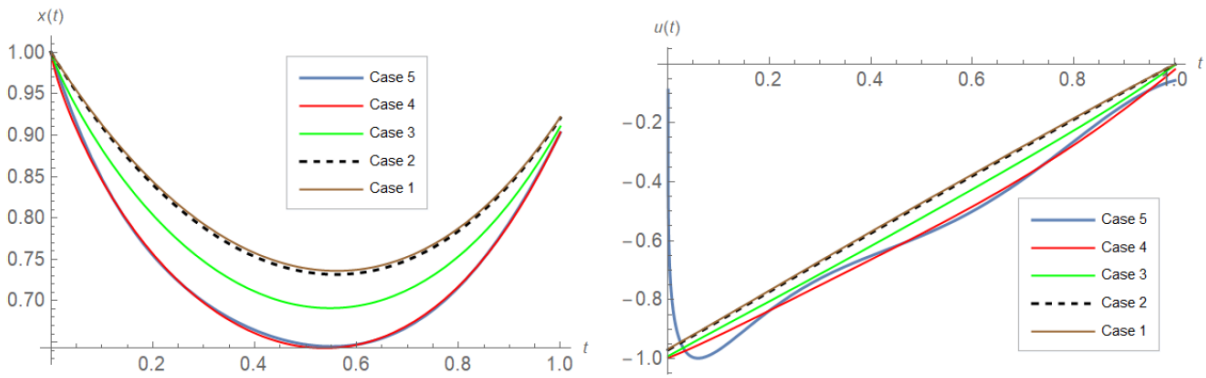

Figure 4.3

Approximate functions of $x(t)$ (left), and $u(t)$ (right) for different distribution functions for Example 4.3.3

Table 4.6

Comparison of approximate values of J for several distribution functions for Example 4.3.2

$\rho(\mu)$	Case 1	Case 2	Case 3	Case 4	Case 5	Case 6
LCM [110]	0.192909	-	0.179690	0.167347	0.165906	-
BWM ($k = 2, M = 5$)[79]	0.183102	0.181852	0.169226	0.153519	0.144717	0.118702
CWM ($k = 1, M = 4$) [90]	0.192921	0.19155	0.179641	0.167328	-	-
LaWM ($k = 1, M = 4$) [90]	0.192604	0.19169	0.185942	0.181798	-	-
CASWM ($k = 1, M = 4$) [90]	0.196914	0.192572	0.180555	0.168072	-	-
LWM ($k = 1, M = 4$) [90]	0.192909	0.191531	0.179529	0.167078	-	-
ADM [111]	0.192909	0.19155	0.17962	0.16740	-	-
VIM [5]	0.192909	0.19153	0.17953	0.16711	-	-
Present method						
$k = 1, M = 4$	0.1929094450240	0.19153090	0.179533	0.167098	0.173066	0.149310
$k = 1, M = 5$	0.1929092989576	0.19153064	0.179529	0.167083	0.172006	0.144279
$k = 1, M = 6$	0.1929092980957	0.19153063	0.179528	0.167078	0.171469	0.141306
$k = 2, M = 4$	0.1929092987957	0.19152875	0.179527	0.167078	0.168267	0.141700
$k = 2, M = 5$	0.1929092980941	0.19152755	0.179524	0.167072	0.167465	0.139448
$k = 2, M = 6$	0.1929092980931	0.19152723	0.179523	0.167072	0.167464	0.139098
J **exact**	0.1929092980931					

Table 4.7

Approximate values of J for distribution functions given in Eq. (4.15) for Example 4.3.3

$\rho(\mu)$	Case 1	Case 2	Case 3	Case 4	Case 5	Case 6
LCM ($\mathcal{M} = 15$) [110]	0.484268	-	0.476446	0.460500	0.451530	-
BWM ($k = 2, M = 5$) [79]	0.399662	0.399579	0.389403	0.364130	0.351287	0.319455
CWM ($k = 1, M = 4$) [90]	0.484232	0.48343	0.475881	0.467005	-	-
LaWM ($k = 1, M = 4$) [90]	0.483476	0.482572	0.473351	0.459714	-	-
CASWM ($k = 1, M = 4$) [90]	0.500511	0.499755	0.492513	0.483723	-	-
LWM ($k = 1, M = 4$) [90]	0.484268	0.483463	0.475886	0.466993	-	-
VIM [5]	0.48426	0.48346	0.47593	0.46722	-	-
Present method						
$k = 1, M = 4$	0.484268503082	0.48346356	0.4758855	0.4669872	0.467826	0.445432
$k = 1, M = 5$	0.484267696480	0.48346265	0.4758827	0.4669781	0.467182	0.442661
$k = 1, M = 6$	0.484267696237	0.48346265	0.4758827	0.4669781	0.467054	0.442106
$k = 2, M = 4$	0.484267707008	0.48340658	0.4758169	0.466901	0.467053	0.442717
$k = 2, M = 5$	0.484267696228	0.48333266	0.4757263	0.466787	0.466603	0.441134
$k = 2, M = 6$	0.484267696228	0.48328334	0.4756663	0.466712	0.466523	0.440962

Table 4.8

Comparison between the obtained J values for distribution functions given in Eq. (4.15) for Example 4.3.4

$\rho(\mu)$	Case 1	Case 2	Case 3	Case 4	Case 5	Case 6
BWM [79]	0.380797	0.379459	0.367210	0.353386	0.364870	0.310670
$(k = 2, M = 5)$						
Present method						
$k = 1, M = 4$	0.38079708031618	0.379407283	0.3667054	0.352312	0.352994	0.312932
$k = 1, M = 5$	0.38079707800506	0.379407283	0.3667052	0.352311	0.352758	0.311821
$k = 1, M = 6$	0.38079707797789	0.379407282	0.3667052	0.352310	0.352607	0.311561
$k = 2, M = 4$	0.38079707798995	0.37938532	0.3666534	0.3522844	0.352654	0.311132
$k = 2, M = 5$	0.38079707797788	0.37937273	0.3666215	0.3522649	0.352499	0.310395
$k = 2, M = 6$	0.38079707797788	0.37935726	0.3665842	0.3522463	0.352463	0.310155
***J* exact**	0.38079707797788					

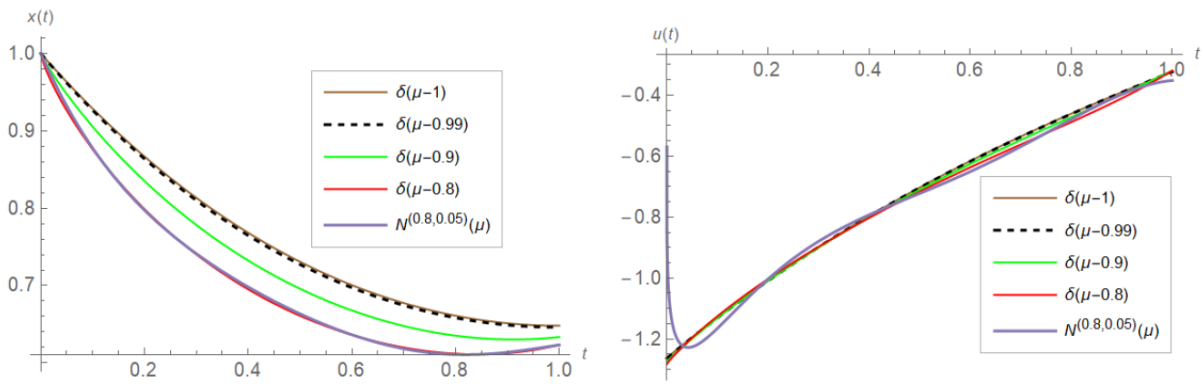

Figure 4.4

Graphs of the approximate functions of $x(t)$ and $u(t)$ with $k = 2, M = 4$ for various choices of distribution function for Example 4.3.4

Table 4.9

Comparison of AE values of $x(t)$ and $u(t)$ for $\rho(\mu) = \delta(\mu - 1)$ for Example 4.3.4

	Present method ($k = 1, M = 10$)		BWM ($k = 1, M = 10$) [79]	
t	$e_{x(t)}$	$e_{u(t)}$	$e_{x(t)}$	$e_{u(t)}$
0.1	1.29×10^{-15}	1.61×10^{-13}	2.39×10^{-13}	2.94×10^{-11}
0.2	1.96×10^{-15}	1.32×10^{-13}	5.01×10^{-12}	4.27×10^{-11}
0.3	5.33×10^{-15}	5.80×10^{-14}	4.05×10^{-12}	4.24×10^{-11}
0.4	5.19×10^{-15}	5.81×10^{-14}	2.63×10^{-12}	2.09×10^{-11}
0.5	4.20×10^{-16}	1.24×10^{-13}	6.16×10^{-12}	2.39×10^{-11}
0.6	5.08×10^{-15}	7.22×10^{-14}	5.95×10^{-12}	2.69×10^{-11}
0.7	5.07×10^{-15}	4.01×10^{-14}	4.81×10^{-12}	1.24×10^{-11}
0.8	2.58×10^{-15}	1.15×10^{-13}	7.83×10^{-12}	1.93×10^{-11}
0.9	1.17×10^{-15}	1.44×10^{-13}	7.07×10^{-12}	1.95×10^{-11}

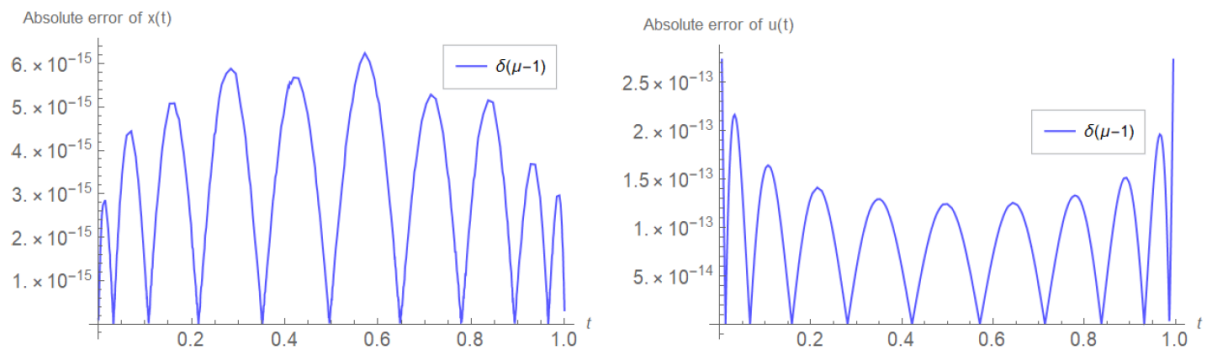

Figure 4.5

Graphs of the AE functions of $x(t)$ and $u(t)$ with $k = 2, M = 4$, at $\rho(\mu) = \delta(\mu - 1)$ for Example 4.3.4

CHAPTER V

VARIABLE-ORDER FRACTIONAL OPTIMAL CONTROL PROBLEMS

VO-FOCPs can be considered as a kind of FOCPs dealing with variable-order fractional derivative operator in their dynamic system, *i.e.* order of the derivative operator is allowed to take any given function. Variable-order operators have memory property, therefore, they have become a powerful tool for modeling complex systems in science and engineering and there has been a growing interest in solving problems containing variable-order fractional derivatives. Several schemes have been developed to find numerical solutions of such problems, for instance, Chebyshev cardinal function method in [40], transcendental Bernstein series method in [33], and Legendre wavelet method in [38].

5.1 Problem statement

Consider the following VO-FOCP

$$\min \quad J(x,u) = \int_0^1 F\left(t, x(t), u(t)\right)\, dt, \tag{5.1}$$

subject to the variable-order fractional dynamical system

$$D^{\beta(t)}x(t) = G(t, x(t), u(t)), \quad n-1 < \beta(t) \leq n, \quad t \in [0,1], \tag{5.2}$$

with

$$x^{(k)}(0) = \lambda_k, \quad k = 0, 1, 2, ..., n-1, \tag{5.3}$$

where F and G are given functions, λ_k for $k = 0, 1, 2, ..., n-1$ are real constants, and n is a positive integer. The problem is to minimize/maximize the functional cost J in Eq. (5.1) subject to Eqs. (5.2) and (5.3). The existence and uniqueness of this problem has been discussed in [9].

5.2 Method of solution

First, we approximate $D^n x(t)$ and $u(t)$ by using (2.5) to obtain

$$D^n x(t) \simeq C^T \Psi^{h,\alpha}_{k,M}(t), \tag{5.4}$$

and

$$u(t) \simeq E^T \Psi^{h,\alpha}_{k,M}(t), \tag{5.5}$$

where $\Psi^{h,\alpha}_{k,M}(t)$ is given in Eq. (2.7), and C and E are unknown constants given by

$$C = [c_{1,0}, ..., c_{1,M}, c_{2,0}, ..., c_{2,M}, ..., c_{2^{k-1},0}, ..., c_{2^{k-1},M}]^T,$$

$$E = [e_{1,0}, ..., e_{1,M}, e_{2,0}, ..., e_{2,M}, ..., e_{2^{k-1},0}, ..., e_{2^{k-1},M}]^T.$$

By applying I^n in Eq. (5.4) and using Proposition 1, we have

$$x(t) \simeq C^T I^n \Psi^{h,\alpha}_{k,M}(t) + \sum_{k=0}^{n-1} \frac{\lambda_k}{k!} t^k. \tag{5.6}$$

Next, by applying $D^{\beta(t)}$ in Eq. (5.6) and using Proposition 1, we get:

$$D^{\beta(t)} x(t) \simeq C^T I^{n-\beta(t)} \Psi^{h,\alpha}_{k,M}(t) + \sum_{k=0}^{n-1} \frac{\lambda_k}{k!} D^{\beta(t)}(t^k), \tag{5.7}$$

where

$$D^{\beta(t)}(t^k) = \begin{cases} 0, & \text{if} \quad k < n, \\ \dfrac{\Gamma(k+1)}{\Gamma(k+1-\beta(t))} t^{k-\beta(t)}, & \text{if} \quad k \geq n. \end{cases} \tag{5.8}$$

By substituting Eqs. (5.5) and (5.6) in Eq. (5.1), we can rewrite the functional cost J as

$$J = \int_0^1 F\left(t, C^T I^n \Psi_{k,M}^{h,\alpha}(t) + \sum_{k=0}^{n-1} \frac{\lambda_k}{k!} t^k, E^T \Psi_{k,M}^{h,\alpha}(t)\right) dt, \tag{5.9}$$

which can be determined numerically by using Gauss-Legendre quadrature. Similarly, by using Eqs. (5.5), (5.6) and (5.7) in Eq. (5.2), we can rewrite the constraint as

$$C^T I^{n-\beta(t)} \Psi_{k,M}^{h,\alpha}(t) + \sum_{k=0}^{n-1} \frac{\lambda_k}{k!} D^{\beta(t)}(t^k) = G\left(t, C^T I^n \Psi_{k,M}^{h,\alpha}(t) + \sum_{k=0}^{n-1} \frac{\lambda_k}{k!} t^k, E^T \Psi_{k,M}^{h,\alpha}(t)\right). \tag{5.10}$$

By collocating Eq. (5.10) at the Newton-Cotes nodes defined by

$$t_i = \frac{2i-1}{2^k\,(M+1)}, \quad i = 1, \ldots, 2^{k-1}\,(M+1), \tag{5.11}$$

we obtain the following system of algebraic constraints

$$\begin{aligned} W_i =& C^T I^{n-\beta(t)} \Psi_{k,M}^{h,\alpha}(t_i) + \sum_{k=0}^{n-1} \frac{\lambda_k}{k!} D^{\beta(t)}(t^k)|_{t=t_i} \\ & - G\left(t_i, C^T I^n \Psi_{k,M}^{h,\alpha}(t_i) + \sum_{k=0}^{n-1} \frac{\lambda_k}{k!} t_i^k, E^T \Psi_{k,M}^{h,\alpha}(t_i)\right) = 0, \quad i = 1, \ldots, 2^{k-1}(M+1). \end{aligned} \tag{5.12}$$

The given VO-FOCP has now been reduced to the following optimization problem: Find the unknown constants C and E so that J in Eq. (5.9) is minimized/maximized subject to the system given in Eq. (5.12).

To solve the obtained parameter optimization problem, we let

$$J^* = J + \Lambda^T W,$$

where

$$\Lambda = [\lambda_{1,0}, ..., \lambda_{1,M}, \lambda_{2,0}, ..., \lambda_{2,M}, ..., \lambda_{2^{k-1},0}, ..., \lambda_{2^{k-1},M}]^T,$$

is the vector of unknown Lagrange multipliers, and

$$W = [W_1, \ldots, W_{2^{k-1}(M+1)}],$$

is a vector containing the algebraic constraints given in Eq. (5.12). The necessary conditions for the optimality of this problem is given by:

$$\frac{\partial J^*}{\partial C} = \frac{\partial J^*}{\partial E} = \frac{\partial J^*}{\partial \Lambda} = 0. \tag{5.13}$$

The above system contains $3(M+1)2^{k-1}$ algebraic equations in $3(M+1)2^{k-1}$ unknown constants. By solving Eq. (5.13), the unknown vectors C, E and Λ can be calculated. Hence, $x(t), u(t)$, and J can be calculated.

5.3 Illustrative examples

Example 5.3.1. Consider the following VO-FOCP [27], [98]

$$min \quad J(x,u) = \int_0^1 \left(t\,u(t) - (\beta(t)+2)\,x(t)\right)^2 dt, \tag{5.14}$$

subject to

$$\dot{x}(t) + D^{\beta(t)}x(t) = t^2 + u(t), \quad 0 < \beta(t) \leq 1, \tag{5.15}$$

with the boundary conditions $x(0) = 0$, and $x(1) = \frac{2}{\Gamma(\beta(1)+3)}$. The exact solutions are

$$x(t) = \frac{2t^{\beta(t)+2}}{\Gamma(\beta(t)+3)}, \quad u(t) = \frac{2t^{\beta(t)+1}}{\Gamma(\beta(t)+2)}. \tag{5.16}$$

This example was considered in [27], and in [98] by using fractional order Bessel wavelets, and Legendre spectral-collocation method respectively, with $\beta(t) = 0.5$ and 1. As [27], we use the same $\beta(t)$ for our method.

In case $\beta(t) = 1$, we use our method with $\alpha = k = 1$ and $M = 2$. First, we approximate $\dot{x}(t)$ and $u(t)$ by using GFOCW as

$$\dot{x}(t) \simeq C^T \Psi_{1,2}^{1,1}(t),$$

and

$$u(t) \simeq E^T \Psi_{1,2}^{1,1}(t), \tag{5.17}$$

where C and E are unknown constants and

$$\Psi_{1,2}^{1,1}(t) = \left[\sqrt{\frac{2}{\pi}}, \frac{-4 + 8t}{\sqrt{\pi}}, \frac{6 - 32t + 32t^2}{\sqrt{\pi}} \right]^T. \tag{5.18}$$

Then,

$$x(t) \simeq C^T I^1 \Psi_{1,2}^{1,1}(t), \tag{5.19}$$

$$D^{\beta(t)} x(t) \simeq C^T I^{1-\beta(t)} \Psi_{1,2}^{1,1}(t), \tag{5.20}$$

where

$$I^1 \Psi_{1,2}^{1,1}(t) = \left[\sqrt{\frac{2}{\pi}}\, t, \frac{4t(t-1)}{\sqrt{\pi}}, \frac{2t(3-4t)^2}{3\sqrt{\pi}} \right]^T. \tag{5.21}$$

By using Eqs. (5.14), (5.17) and (5.19), we get

$$J = \int_0^1 \left(t\, E^T \Psi_{1,2}^{1,1}(t) - (\beta(t) + 2)\, C^T I^1 \Psi_{1,2}^{1,1}(t) \right)^2 dt, \tag{5.22}$$

from which J can be evaluated numerically in terms of C and E. By substituting Eqs. (5.17), (5.19) and (5.20) in Eq. (5.15), and collocating the resulting equation at the nodes given in Eq. (5.11), we obtain a system of equations as

$$C^T \Psi_{1,2}^{1,1}(t_i) + C^T I^{1-\beta(t)} \Psi_{1,2}^{1,1}(t_i) = t_i^2 + E^T \Psi_{1,2}^{1,1}(t_i), \qquad i = 1, \ldots, 2^{k-1}(M+1). \tag{5.23}$$

Hence we have the parameter optimization problem given by: Find the unknown constants C and E which minimize the cost J given in Eq. (5.22) subject to the constraints given in Eq. (5.23). By solving this optimization problem, we obtain

$$C = E = \left[\frac{5\sqrt{2\pi}}{32}, \frac{\sqrt{\pi}}{8}, \frac{\sqrt{\pi}}{32}\right]^T,$$

from which we obtain $x(t) = \frac{1}{3}x^3$, $u(t) = x^2$, and $J = 0$ which are the exact solutions.

In case $\beta(t) = 0.5$, we use $\alpha = 0.5$, $k = 1$, and $M = 3$. In this case, we write

$$\dot{x}(t) \simeq C_1^T \Psi_{1,3}^{1,0.5}(t),$$

and

$$u(t) \simeq E_1^T \Psi_{1,3}^{1,0.5}(t), \tag{5.24}$$

where C_1 and E_1 are unknown constants. By using the similar procedure as $\beta(t) = 1$, we get

$$C_1 = E_1 = \left[\frac{7}{12\sqrt{2}}, \frac{7}{24}, \frac{1}{8}, \frac{1}{48}\right]^T.$$

From these, we have $x(t) = \frac{2x^{3.5}}{\Gamma(4.5)}$, $u(t) = \frac{2x^{2.5}}{\Gamma(3.5)}$, and $J = 0$ which are the exact solutions again. These exact solutions were not obtained in [27] and [98].

Example 5.3.2. Consider [27]:

$$min \quad J(x,u) = \int_0^1 (u(t) - x(t))^2 \, dt, \tag{5.25}$$

subject to

$$\dot{x}(t) + D^{\beta(t)}x(t) = -x(t) + u(t) + t^3 + \frac{6\, t^{\beta(t)+2}}{\Gamma(\beta(t)+3)}, \quad 0 < \beta(t) \leq 1,$$
$$x(0) = 0, \quad x(1) = \frac{6}{\Gamma(\beta(1)+4)}.$$

The exact solutions are $x(t) = u(t) = \frac{6\,t^{\beta(t)+3}}{\Gamma(\beta(t)+4)}$, with the corresponding optimal $J = 0$. This problem was solved in [27] for several values of $\beta(t)$. We use the same values of $\beta(t)$ as in [27].

In case $\beta(t) = 1$, by setting $\alpha = 1$, $k = 1$, and $M = 4$, we obtain

$$C = \left[\frac{7\sqrt{2\pi}}{64}, \frac{7\sqrt{\pi}}{64}, \frac{3\sqrt{\pi}}{64}, \frac{\sqrt{\pi}}{128}, 0\right]^T,$$
$$E = \left[\frac{21\sqrt{2\pi}}{1024}, \frac{3\sqrt{\pi}}{128}, \frac{27\sqrt{\pi}}{2048}, \frac{\sqrt{\pi}}{256}, \frac{\sqrt{\pi}}{2048}\right]^T,$$

which yields $x(t) = u(t) = \frac{x^4}{4}$ and the optimal cost functional $J = 0$.

Similarly, in case $\beta(t) = 0.5$, we solve this example with $\alpha = 0.5,\ k = 1$ and $M = 7$. We obtain the unknown constants as

$$C_1 = \left[\frac{33}{80\sqrt{2}}, \frac{33}{128}, \frac{11}{64}, \frac{11}{160}, \frac{1}{64}, \frac{1}{640}, 0, 0\right]^T,$$
$$E_1 = \left[\frac{143}{1792\sqrt{2}}, \frac{143}{2560}, \frac{177}{2560}, \frac{13}{512}, \frac{5}{512}, \frac{9}{3584}, \frac{1}{2560}, \frac{1}{35840}\right]^T.$$

Therefore, we get $x(t) = u(t) = \frac{32x^{3.5}}{35\sqrt{\pi}}$ and the minimal cost $J = 0$ which are the exact solutions. These exact solutions were not obtained in [27] and [73].

In addition, in Table 5.1 on page 71, we compare the absolute errors (AEs) of $x(t)$ and $u(t)$ by using the method in [27], and our method with $\alpha = 0.5$, $k = 2$, $M = M_2 = 7$, $\beta(t) = 0.47$ and 0.49. In Table 5.2 on page 72, we give the values of J obtained in [27] and calculated by our method for $\beta(t) = 0.8 + 0.05\,sin(t)$, $0.8 + 0.005\,sin(t)$ and $0.8 + 0.0005\,sin(t)$.

Example 5.3.3. Consider [38]

$$min \quad J(x,u) = \int_0^1 \left(e^t\left(x(t) + t - t^4 - 1\right)^2 + (1+t^2)\left(u(t) + t^4 - t + 1 - \frac{24\,t^{4-\beta(t)}}{\Gamma(5-\beta(t))}\right)^2\right) dt, \tag{5.26}$$

subject to

$$D^{\beta(t)} = u(t) + x(t), \quad 1 < \beta(t) \leq 2, \tag{5.27}$$

with $x(0) = 1, \dot{x}(0) = -1$.

The exact solutions are

$$x(t) = t^4 - t + 1, \quad u(t) = \frac{24\, t^{4-\beta(t)}}{\Gamma(5 - \beta(t))} - (t^4 - t + 1).$$

These values give the optimal performance index $J = 0$. The authors in [38] used the Legendre wavelets with $k = 2$ and $M_1 = 10$ to solve this example with different values of $\beta(t) = \beta_i(t)$ given by

$$\beta_1(t) = 1.9, \qquad \beta_4(t) = 1.5 + 0.15\, sin(2\pi t),$$

$$\beta_2(t) = 1.9 - 0.2\, t^2, \qquad \beta_5(t) = 1.5 + 0.25\, sin(2\pi t),$$

$$\beta_3(t) = 1.9 - 0.4\, t^2, \qquad \beta_6(t) = 1.5 + 0.45\, sin(2\pi t).$$

In Table 5.3 on page 72, we give a comparison between the maximal AE values for $x(t), u(t)$ and J obtained by using our method with $\alpha = 1, k = 1$ and $M = 2$ by selecting the same values of $\beta(t)$ by those from [38]. In this table, the CPU times for computing the solution is also included. In addition, figure 5.1 on the next page displays the behavior of the obtained approximate functions for $u(t)$ with different values of $\beta(t)$ with $k = 1$, and $M = 2$. Absolute error function of $x(t)$ at two distribution functions $\beta_3(t) = 1.9 - 0.4\, t^2$ and $\beta_6(t) = 1.5 + 0.45\, sin(2\pi t)$, are given in figure 5.2 on page 68.

Example 5.3.4. Consider [33]

$$min \quad J(x,u) = \int_0^1 \left(\left(x(t) - t^2 \right)^2 + \left(u(t) + t^4 - \frac{2}{\Gamma(3 - \beta(t))} t^{2-\beta(t)} \right)^2 \right) dt, \tag{5.28}$$

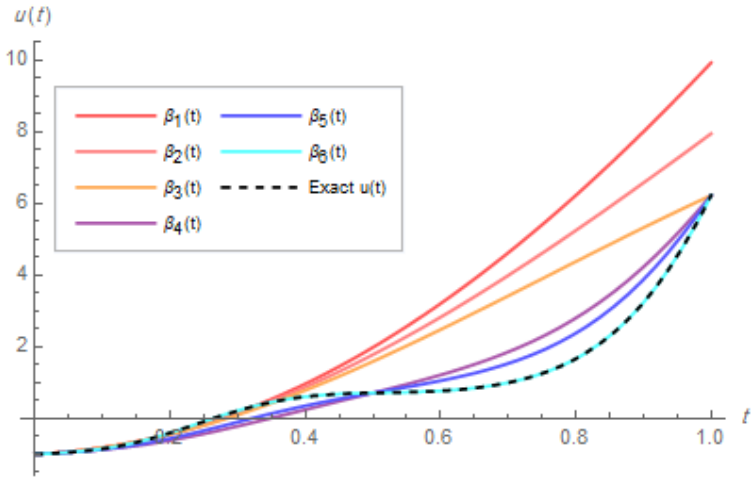

Figure 5.1

Approximate functions of $u(t)$ at several values of $\beta(t)$ with $\alpha = 1$, $k = 1$, and $M = 2$, for Example 5.3.3

subject to

$$D^{\beta(t)}x(t) = u(t) + t^2\,x(t), \quad 1 < \beta(t) \leq 2,$$

with

$$x(0) = \dot{x}(0) = 0.$$

The exact solutions are

$$x(t) = t^2, \quad u(t) = \frac{2}{\Gamma(3-\beta(t))}t^{2-\beta(t)} - t^4, \quad \text{and } J = 0.$$

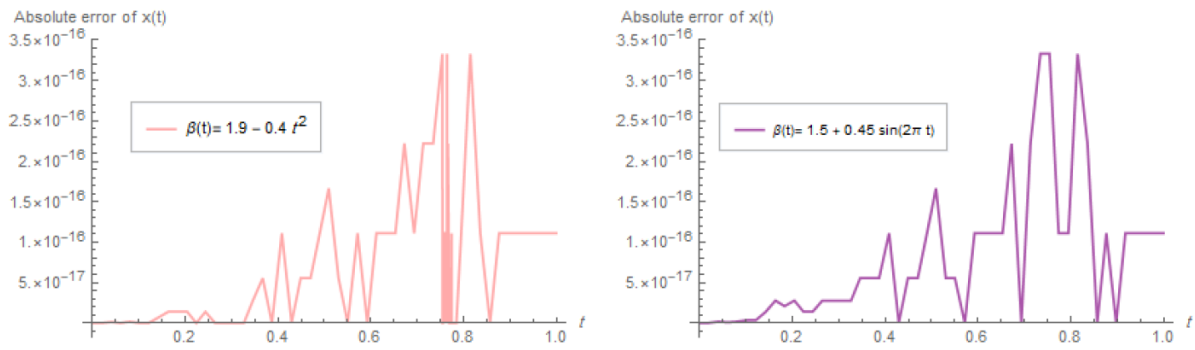

Figure 5.2

Plots of AE functions of $x(t)$ for $\beta_3(t)$, and $\beta_6(t)$ with $\alpha = 1$, $k = 1$, and $M = 3$, for Example 5.3.3

This problem was solved in [33] by using the transcendental Bernstein series (TBS) method by selecting degree $m_1 = 3$ to approximate $x(t)$ and degree $m_2 = 5$ to approximate $u(t)$ with the following $\beta(t) = \beta_i(t)$:

$$\beta_1(t) = 1.1, \qquad \beta_3(t) = 1.1 + 0.0004\, e^{t^3},$$

$$\beta_2(t) = 1.1 + 0.001\cos(t^2), \qquad \beta_4(t) = 1.1 + 0.006\,|t-1|\sin^2(t).$$

In Table 5.4 on page 72, we give a comparison between the calculated AE values for J by using our method with $\alpha = 1, k = 1, M = 2$, and by selecting the same values of $\beta(t)$ from the TBS method. In addition, in figure 5.3 on the following page, we give AEs for $x(t), u(t)$ with $\beta(t) = \beta_2(t)$ which is the same value as figure 2 in Ref. [33]. We see in our figure that the AEs for $x(t)$ and $u(t)$ are multiples of 10^{-17} and 10^{-16}, respectively. However, the AE errors for $x(t)$ and $u(t)$ in the figure of the same problem in [33] are multiples of 10^{-9} and 10^{-5}.

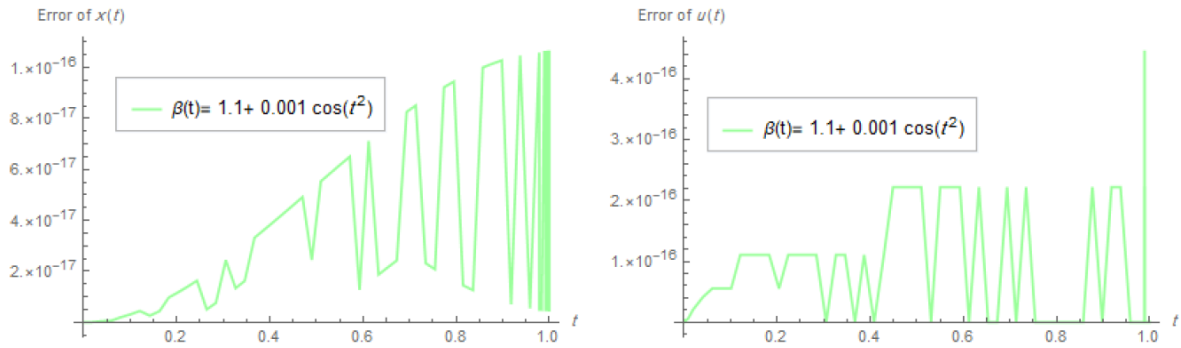

Figure 5.3

The AE functions of $x(t)$ (left), and $u(t)$ (right) for $\beta(t) = \beta_2(t)$ for Example 5.3.4

Example 5.3.5. Consider [33]

$$min \quad J(x,u) = \int_0^1 \left(\left(x(t) - t^{\frac{3}{2}} \right)^2 + \left(u(t) - \left(0.5\, e^{-t} \left(\frac{3\sqrt{\pi}}{4\Gamma(\frac{5}{2} - \beta(t))} t^{\frac{3}{2} - \beta(t)} - e^{t^{\frac{3}{2}}} \right) \right) \right)^2 \right) dt, \tag{5.29}$$

subject to

$$D^{\beta(t)} x(t) = 2\, e^t u(t) + e^{x(t)}, \quad 0 < \beta(t) \leq 1, \tag{5.30}$$

and $x(0) = 0$.

From [33], the optimal value of the performance index is $J = 0$, which is achieved by

$$x(t) = t^{\frac{3}{2}}, \text{ and } u(t) = 0.5\, e^{-t} \left(\frac{3\sqrt{\pi}}{4\Gamma(\frac{5}{2} - \beta(t))} t^{\frac{3}{2} - \beta(t)} - e^{t^{\frac{3}{2}}} \right). \tag{5.31}$$

This problem was solved in [33] by using the TBS method with $m_1 = m_2 = 4$ and the following $\beta(t) = \beta_i(t)$:

$$\beta_1(t) = 1, \qquad \beta_3(t) = 1 - 0.01e^t,$$

$$\beta_2(t) = 1 - \frac{e^t cos(t)}{30}, \qquad \beta_4(t) = 1 - \frac{cos^3(t)}{50}.$$

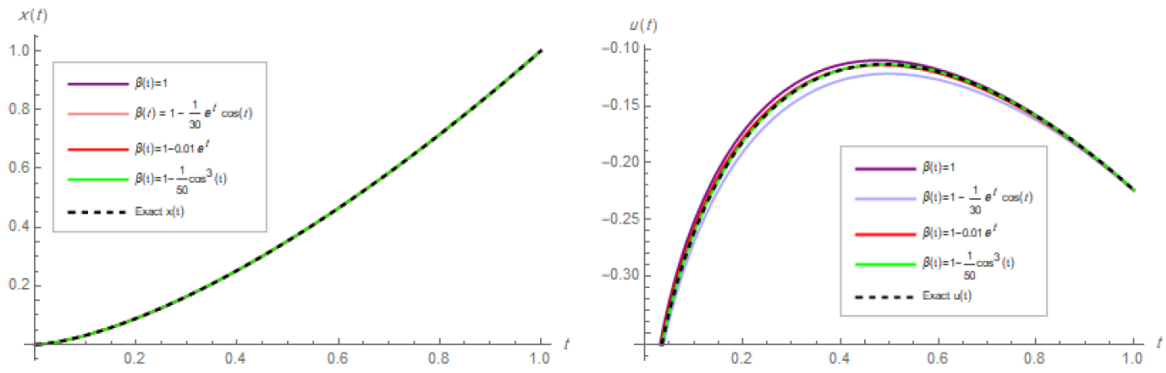

Figure 5.4

Approximate functions of $x(t)$ (left), and $u(t)$ (right) for several values of $\beta(t)$ along with the exact solution for Example 5.3.5

A comparison between the numerical values for J calculated by our method with $\alpha = 0.5$, $k = 1$, $M = 2$ and those at the same values of $\beta(t)$ from TBS method are presented in Table 5.5 on page 73. In figure 5.4, the graphs of the exact $x(t)$ and $u(t)$ given in Eq. (5.31) together with the graphs of the numerical solutions for $x(t)$ and $u(t)$ obtained by our method are presented. In figure 5.5 on the next page, the AEs of $x(t)$ and $u(t)$ for $\beta(t) = \beta_2(t)$ are plotted.

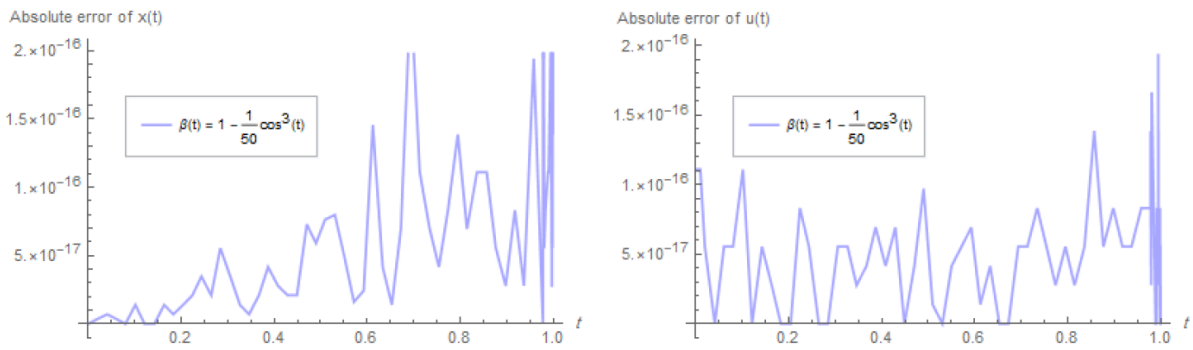

Figure 5.5

The AEs of $x(t)$ (left), and $u(t)$ (right) for $\beta(t) = \beta_2(t)$ for Example 5.3.5

Table 5.1

Comparison of AE values of $x(t)$ and $u(t)$ with $\alpha = 0.5$, $k = 2$, and $M = M_2 = 7$ for Example 5.3.2

	$e_{x(t)}$				$e_{u(t)}$			
t	$\beta(t) = 0.47$		$\beta(t) = 0.49$		$\beta(t) = 0.47$		$\beta(t) = 0.49$	
	Present method	BW method	Present method	BW method	Present method	BW method	Present method	BW method
0.1	4.55×10^{-11}	9.26×10^{-5}	1.44×10^{-11}	3.24×10^{-5}	3.12×10^{-10}	9.26×10^{-5}	9.28×10^{-11}	3.24×10^{-5}
0.2	3.75×10^{-11}	1.19×10^{-4}	1.19×10^{-11}	4.18×10^{-5}	1.33×10^{-9}	1.20×10^{-4}	4.27×10^{-10}	4.20×10^{-5}
0.3	1.15×10^{-11}	1.36×10^{-4}	3.67×10^{-12}	4.78×10^{-5}	1.13×10^{-10}	1.35×10^{-4}	3.83×10^{-11}	4.73×10^{-5}
0.4	2.27×10^{-12}	1.49×10^{-4}	6.21×10^{-13}	5.23×10^{-5}	4.11×10^{-11}	1.50×10^{-4}	1.34×10^{-11}	5.26×10^{-5}
0.5	1.12×10^{-11}	3.46×10^{-5}	3.62×10^{-12}	1.20×10^{-5}	3.85×10^{-11}	3.46×10^{-5}	1.30×10^{-11}	1.20×10^{-5}
0.6	2.23×10^{-12}	2.53×10^{-5}	6.43×10^{-13}	8.85×10^{-6}	1.11×10^{-10}	2.53×10^{-5}	3.75×10^{-11}	8.85×10^{-6}
0.7	3.95×10^{-12}	1.75×10^{-5}	1.23×10^{-12}	6.15×10^{-6}	1.26×10^{-10}	1.75×10^{-5}	4.23×10^{-11}	6.15×10^{-6}
0.8	9.53×10^{-12}	1.09×10^{-5}	3.10×10^{-12}	3.82×10^{-6}	3.42×10^{-11}	1.09×10^{-5}	1.16×10^{-11}	3.82×10^{-6}
0.9	2.79×10^{-13}	5.12×10^{-6}	1.57×10^{-14}	1.79×10^{-6}	2.50×10^{-11}	5.12×10^{-6}	8.57×10^{-12}	1.79×10^{-6}

Table 5.2

Numerical values of J with $\alpha = 0.5$, at some functions of $\beta(t)$ for Example 5.3.2

$\beta(t)$	$0.8 + 0.05\,sin(t)$	$0.8 + 0.005\,sin(t)$	$0.8 + 0.0005\,sin(t)$
Present method	2.08331×10^{-15}	4.96459×10^{-17}	2.20447×10^{-17}
BW method	7.9873×10^{-10}	3.3543×10^{-10}	3.0794×10^{-10}

Table 5.3

Comparison of maximal AEs of the obtained $J, x(t)$, and $u(t)$ at different functions of $\beta(t)$ for Example 5.3.3

$\beta(t)$	Present method ($k = 1$, $M = 2$)				LW method ($k = 2$, M_1=10) [38]			
	$e_{x(t)}$	$e_{u(t)}$	e_J	CPU(s)	$e_{x(t)}$	$e_{u(t)}$	e_J	CPU(s)
$\beta_1(t)$	5.551×10^{-17}	2.401×10^{-15}	1.058×10^{-30}	2.11	5.792×10^{-5}	6.599×10^{-6}	3.329×10^{-9}	11.49
$\beta_2(t)$	3.885×10^{-16}	3.775×10^{-15}	5.539×10^{-31}	2.42	4.421×10^{-5}	4.902×10^{-6}	1.868×10^{-9}	11.63
$\beta_3(t)$	3.885×10^{-16}	1.998×10^{-15}	5.675×10^{-31}	2.55	3.369×10^{-5}	3.676×10^{-6}	1.084×10^{-9}	12.85
$\beta_4(t)$	4.302×10^{-16}	1.221×10^{-15}	6.455×10^{-31}	2.46	5.994×10^{-6}	1.110×10^{-6}	5.900×10^{-11}	13.50
$\beta_5(t)$	2.914×10^{-16}	8.465×10^{-16}	4.614×10^{-31}	2.69	6.532×10^{-6}	1.101×10^{-6}	9.014×10^{-11}	12.94
$\beta_6(t)$	1.110×10^{-16}	2.664×10^{-15}	2.577×10^{-31}	2.63	9.389×10^{-6}	1.304×10^{-6}	2.894×10^{-10}	12.77

Table 5.4

Comparison between the numerical values of J for Example 5.3.4

$\beta(t)$	Present method ($k = 1, M = 2$)	TBS ($m_1 = 3, m_2 = 5$) [33]
$\beta_1(t)$	5.78561×10^{-32}	2.42964×10^{-19}
$\beta_2(t)$	1.47523×10^{-32}	3.75371×10^{-17}
$\beta_3(t)$	7.63644×10^{-32}	1.50544×10^{-19}
$\beta_4(t)$	3.70426×10^{-32}	2.91502×10^{-18}

Table 5.5

The numerical values of J for Example 5.3.5

$\beta(t)$	Present method	TBS method [33]
1	5.96750×10^{-33}	1.64830×10^{-8}
$1 - \frac{e^t cos(t)}{30}$	7.71312×10^{-33}	1.96391×10^{-8}
$1 - 0.01e^t$	7.16928×10^{-33}	1.37496×10^{-8}
$1 - \frac{cos^3(t)}{50}$	1.00063×10^{-33}	5.72515×10^{-9}

CHAPTER VI

CONCLUSIONS

A general formulation for calculating the exact value of the Riemann-Liouville fractional integral operator (RLFIO) for the generalized fractional-order Chebyshev wavelets (GFOCW) has been derived. The GFOCW, and the RLFIO were applied to approximate the numerical solution of the fractional-order optimal control problems containing both equality and inequality constraints, distributed-order fractional optimal control problems, and variable-order fractional optimal control problems. Some key features of the proposed method are as follows:

- We could obtain the exact value of the Riemann-Liouville fractional integral operator for Generalized fractional-order Chebyshev wavelets.
- The proposed method could obtain the exact solutions of some problems whose exact solutions are polynomials or fractional-order monomials. These exact solutions were not obtained previously in the literature.
- Our numerical method gives more accurate solutions than those shown in the literature.

6.1 For Further Research

We plan to extend this method to fractional-order partial differential equations and two-dimensional fractional-order differential equations.

REFERENCES

[1] M. Abramowitz and I. A. Stegun, *Handbook of Mathematical Functions*, Washington: National Bureau of Standards 1965, 1973.

[2] O. P. Agrawal and D. Baleanu,"A Hamiltonian formulation and a direct numerical scheme for fractional optimal control problems", *J. Vib. Control*, vol. 13, no. 9-10, 2007, pp. 1269-1281.

[3] W. G. Aiello, H. I. Freedman, and J. Wu, "Analysis of a model representing stage-structured population growth with state-dependent time delay", *SIAM J. Appl. Math.*, vol. 52, no. 3, 1992, pp. 855-869.

[4] M. Alipour, D. Rostamy, and D. Baleanu, "Solving multi-dimensional fractional optimal control problems with inequality constraint by Bernstein polynomials operational matrices", *J. Vib. Control*, vol. 19, no. 16 , 2013, pp. 2523-2540.

[5] A. Alizadeh and S. Effati, "An iterative approach for solving fractional optimal control problems", *J. Vib. Control*, vol. 24, no. 1, 2018, pp. 18-36.

[6] T. M. Atanackovic, "A generalized model for the uniaxial isothermal deformation of a viscoelastic body", *Acta Mech.*, vol. 159, no. 1, 2002, pp. 77-86.

[7] A. Atangana, "Blind in a commutative world: simple illustrations with functions and chaotic attractors", *Chaos Soliton. Fract.*, vol. 114, 2018, pp. 347-363.

[8] A. Atangana and J. F. Gomez-Aguilar, "Decolonisation of fractional calculus rules: breaking commutativity and associativity to capture more natural phenomena", *Eur. Phys. J. Plus*, vol. 133, no. 4, 2018, pp. 1-22.

[9] G. M. Bahaa, "Fractional optimal control problem for variable-order differential systems", *Fract. Calc. Appl. Anal.*, vol. 20, no. 6, 2017, pp.1447-1470.

[10] H. T. Banks, J. A. Burns, "Hereditary control problems: numerical methods based on averaging approximations", *SIAM J. Control Optim.*, vol. 16, no. 2, 1978, pp. 169-208.

[11] Z. Barikbin and E. Keshavarz, "Solving fractional optimal control problems by new Bernoulli wavelets operational matrices", *Optim. Contr. Appl. Met.*, vol. 41, no. 4, 2020, pp. 1188-1210.

[12] R. F. Bass, "Real analysis for graduate students", Createspace Ind. Pub, 2013.

[13] G. Beylkin, R. Coifman, and V. Rokhlin, "Fast wavelet transforms and numerical algorithms", *Commun. Pur. Appl. Math.*, vol. 44, no. 2, 1991, pp. 141-183.

[14] S. K. Bhatt, "An existence theorem for a fractional control problem", *J. Optimiz. Theory App.*, vol. 11, no. 4, 1973, pp. 379-385.

[15] A. H. Bhrawy and S. Ezz-Eldien, "A new Legendre operational technique for delay fractional optimal control problems", *Calcolo*, vol. 53, no. 4, 2016, pp. 521-543.

[16] A. Bhrawy, Y. Alhamed, D. Baleanu, and A. Al-Zahrani, "New spectral techniques for systems of fractional differential equations using fractional-order generalized Laguerre orthogonal functions", *Frac. Calc. Appl. Anal.*, vol. 17, no. 4, 2014, pp. 1137-1157.

[17] G. W. Bohannan, " Analog fractional order controller in temperature and motor control applications", *J. Vib. Control*, vol. 14, no. 9-10, 2008, pp. 1487-1498

[18] C. Canuto, M. Y. Hussaini, A. Quarteroni, and T. A. Zang, "Spectral Methods-Fundamentals in Single Domains", Springer, Berlin, 2006.

[19] A. V. Chechkin, R. Gorenflo, I. M Sokolov, and V. Y. Gonchar, "Distributed order time fractional diffusion equation", *Fract. Calc. Appl. Anal.*, vol. 6, no. 3, 2003, pp. 259-280.

[20] C. L. Chen, D. Y. Sun, and C. Y. Chang, "Numerical solution of time-delayed optimal control problems by iterative dynamic programming", *Optim. contr. Appl. Met.*, vol. 21, no. 3, 2000, 91-105.

[21] T. Chiranjeevi and R. K. Biswas, "Computational method based on reflection operator for solving a class of fractional optimal control problem", *Procedia Comput. Sci.*, vol. 171, 2020, pp. 2030-2039.

[22] S. Dadebo, and R. Luus, "Optimal control of time-delay systems by dynamic programming", *Optim. Contr. Appl. Met.*, vol. 13, no. 1, 1992, pp. 29-41.

[23] M. Dadkhah and M. H. Farahi, "Optimal control of time delay systems via hybrid of block-pulse functions and orthonormal Taylor series", *Int. J. Appl. Comput. Math.*, vol. 2, no. 1, 2016, pp. 137-152.

[24] W. Dahmen, S. Prößdorf, and R. Schneider, "Wavelet approximation methods for pseudodifferential equations II: Matrix compression and fast solution", *Adv. comput. Math.*, vol. 1, no. 3, 1993, pp. 259-335.

[25] I. Daubechies, "The wavelet transform, time-frequency localization and signal analysis", *IEEE Trans. Inform. Theory*, vol. 36, no. 5, 1990, pp. 961-1005.

[26] H. Dehestani, Y. Ordokhani, and M. Razzaghi, "Fractional-order Bessel wavelet functions for solving variable order fractional optimal control problems with estimation error", *Int. J. Syst. Sci.*, vol. 51, no. 6, 2020, pp. 1032-1052.

[27] H. Dehestani, Y. Ordokhani, and M. Razzaghi, "Fractional-order Bessel wavelet functions for solving variable order fractional optimal control problems with estimation error", *Int. J. Sys. Sci.*, vol. 51, no. 6, 2020, pp. 1032-1052.

[28] S. Effati, S. A. Rakhshan, and S. Saqi, "Formulation of Euler–Lagrange equations for multi-delay fractional optimal control problems", *J. Comput. Nonlin. Dyn.*, vol. 13, no. 6, 2018.

[29] G. Ghanbari and M. Razzaghi, M. (2021). Numerical solutions for fractional optimal control problems by using generalised fractional-order Chebyshev wavelets. *Int. J. Sys. Sci.*, vol. 53, no. 4, 2022, pp. 778-792.

[30] G. Ghanbari and M. Razzaghi, "Fractional-order Chebyshev wavelet method for variable-order fractional optimal control problems", *Math. Method. Appl. Sci.*, vol. 45, no. 2, 2022, pp. 827-842.

[31] G. Ghanbari and M. Razzaghi, "Numerical solutions for distributed-order fractional optimal control problems by using generalized fractional-order Chebyshev wavelets", *Nonlinear Dynam.*, 2022, pp. 1-13.

[32] R. Gorenflo, F. Mainardi, E. Scalas, and M. Raberto, "Fractional calculus and continuous-time finance. III: The diffusion limit", *Math. financ.*, Birkhuser, Basel, 2001, pp. 171-180.

[33] H. Hassani and Z. Avazzadeh, "Transcendental Bernstein series for solving nonlinear variable order fractional optimal control problems", *Appl. Math. Comput.*, vol. 362, 2019, pp. 124563.

[34] N. Haddadi, Y. Ordokhani, and M. Razzaghi, "Optimal control of delay systems by using a hybrid functions approximation", *J. Optimiz. Theory App.*, vol. 153, no. 2, 2012, pp. 338-356.

[35] H. Hassani, J. T. Machado, and E. Naraghirad, "Generalized shifted Chebyshev polynomials for fractional optimal control problems", *Commun. Nonlinear Sci.*, vol. 75, 2019, pp. 50-61.

[36] H. Hassani, J. T. Machado, and S. Mehrabi, "An optimization technique for solving a class of nonlinear fractional optimal control problems: Application in cancer treatment", *Appl. Math. Model.*, vol. 93, 2021, pp. 868-884.

[37] J. H. He, "Nonlinear oscillation with fractional derivative and its applications", *International conference on vibrating engineering*, Vol. 98, 1998, pp. 288-291.

[38] M. H. Heydari and Z. Avazzadeh, "A new wavelet method for variable-order fractional optimal control problems", *Asian J. Control*, vol. 20, 2018, pp. 1804-1817.

[39] M. H. Heydari, M. R. Hooshmandasl, F. M. Ghaini, and C. Cattani, "Wavelets method for solving fractional optimal control problems", *Appl. Math. Comput.*, vol. 286, 2016, pp. 139-154.

[40] M. H. Heydari, "Numerical solution of nonlinear 2D optimal control problems generated by Atangana-Riemann-Liouville fractal-fractional derivative", *Appl. Numer. Math.*, vol. 150, 2020, pp. 507-518.

[41] S. Hosseinpour, A. Nazemi, and E. Tohidi, "Müntz–Legendre spectral collocation method for solving delay fractional optimal control problems", *J. Comput. Appl. Math.*, vol. 351, 2019, pp. 344-363.

[42] C. Ionescu, A. Lopes, D. Copot, J. T. Machado, J. T., and J. H. T. Bates, "The role of fractional calculus in modeling biological phenomena: A review", *Commun. Nonlinear Sci.*, vol. 51, 2017, pp. 141-159.

[43] A. Jajarmi and D. Baleanu, "Suboptimal control of fractional-order dynamic systems with delay argument", *J. Vib. Control*, vol. 24, no. 12, 2018, pp. 2430-2446.

[44] A. Jajarmi and M. Hajipour, "An efficient recursive shooting method for the optimal control of time-varying systems with state time-delay", *Appl. Math. Model.*, vol. 40, no. 4, 2016, pp. 2756-2769.

[45] S. Kazem, S. Abbasbandy, and S. Kumar, "Fractional-order Legendre functions for solving fractional-order differential equations", *Appl. Math. Model.*, vol. 37, no. 7, 2013, pp. 5498-5510.

[46] F. Khellat, "Optimal control of linear time-delayed systems by linear Legendre multiwavelets", *J. optimiz. Theory App.*, vol. 143, no. 1, 2009, pp. 107-121.

[47] F. Khellat and N. Vasegh, "Suboptimal control of linear systems with delays in state and input by orthonormal basis", *Int. J. Comput. Math.*, vol. 88, no, 4, 2011, pp. 781-794.

[48] A.N. Kochubei, "Distributed order calculus and equations of ultraslow diffusion", *J. Math. Anal. Appl.*, vol. 340, 2008, pp. 252–281.

[49] W. Li, S. Wang, and V. Rehbock, "Numerical solution of fractional optimal control", *J. Optimiz. Theory App.*, vol. 180, no. 2, 2019, pp. 556-573.

[50] Y. Li and W. Zhao, "Haar wavelet operational matrix of fractional order integration and its applications in solving the fractional order differential equations", *Appl. Math. Comput.*, vol. 216, no. 8, 2010, pp. 2276-2285.

[51] A. Lotfi, "Epsilon penalty method combined with an extension of the Ritz method for solving a class of fractional optimal control problems with mixed inequality constraints", *Appl. Numer. Math.*, vol. 135, 2019, pp. 497-509.

[52] C.F. Lorenzo and T.T. Hartley, "Variable-order and distributed order fractional operators", *Nonlinear Dynam.*, vol. 29, no. 1, 2002, pp. 57–98.

[53] M. Malek-Zavarei and M. Jamshidi, "Time-delay systems: analysis, optimization and applications", *Elsevier Science Inc.*, 1987.

[54] I. Malmir, "Novel Chebyshev wavelets algorithms for optimal control and analysis of general linear delay models", *Appl. Math. Model.*, vol. 69, 2019, pp. 621-647.

[55] I. Malmir and S. H. Sadati, "Transforming linear time-varying optimal control problems with quadratic criteria into quadratic programming ones via wavelets", *J. Appl. Anal.*, vol. 26, no. 1, 2020, pp. 131-151

[56] H. R. Marzban and F. Malakoutikhah, "Solution of delay fractional optimal control problems using a hybrid of block-pulse functions and orthonormal Taylor polynomials", *J. the Frankl. Inst.*, vol. 356, no. 15, 2019, pp. 8182-8215.

[57] H.R. Marzban and M. Razzaghi , "Optimal control of linear delay systems via hybrid of block-pulse and Legendre polynomials", *J. Frankl. Inst.*, vol. 341, no. 3, 2004, pp. 279–293.

[58] H. R. Marzban, H. R. Tabrizidooz, and M. Razzaghi, "Hybrid functions for nonlinear initial-value problems with applications to Lane-Emden type equations", *Phys. Lett. A*, vol. 372, no. 37, 2008, pp. 5883-5886.

[59] S. Mashayekhi and M. Razzaghi, "Numerical solution of the fractional Bagley-Torvik equation by using hybrid functions approximation", *Math. Method. Appl. Sci.*, vol. 39, no. 3, 2016, pp. 353-365.

[60] S. Mashayekhi and M. Razzaghi, "Numerical solution of distributed order fractional differential equations by hybrid functions", *J. Comput. Phys.*, vol.315, 2016, pp. 169-181.

[61] S. Mashayekhi and M. Razzaghi, "An approximate method for solving fractional optimal control problems by hybrid functions", *J. Vib. Control*, vol. 24, no. 9, 2018, pp. 1621-1631.

[62] M.M. Meerschaert, H.P. Scheffler, "Stochastic model for ultraslow diffusion", *Stoch. Process. Appl.*, vol. 116, no.9, 2006, pp. 1215–1235.

[63] K. S. Miller and B. Ross, *An introduction to the fractional calculus and fractional differential equations*. Wiley.

[64] R. Mohammadzadeh and M. Lakestani, "Optimal control of linear time-delay systems by a hybrid of block-pulse functions and biorthogonal cubic Hermite spline multiwavelets", *Optim. Contr. Appl. Met.*, vol. 39, no. 1, 2018, pp. 357-376.

[65] L. Moradi, F. Mohammadi, and D. Baleanu, "A direct numerical solution of time-delay fractional optimal control problems by using Chelyshkov wavelets", *J. Vib. Control*, vol. 25, no. 2, 2019, pp. 310-324.

[66] A. Nazemi and M. Mansoori, "Solving optimal control problems of the time-delayed systems by Haar wavelet", *J. Vib. Control*, vol. 22, no. 11, 2016, pp. 2657-2670.

[67] A. Nazemi and M. M. Shabani, "Numerical solution of the time-delayed optimal control problems with hybrid functions", *IMA J. Math. Control I.*, vol. 32, no. 3, 2015, pp. 623-638.

[68] S. Nemati, P.M. Lima, and D.F. Torres, "A numerical approach for solving fractional optimal control problems using modified hat functions", *Commun. Nonlinear Sci.*, vol. 78, 2019, pp. 104849.

[69] Z. M. Odibat and N. T. Shawagfeh, "Generalized Taylor's formula", *Appl. Math. Comput.*, vol. 186, no. 1, 2007, pp. 286-293.

[70] K. R. Palanisamy, "Analysis and optimal control of linear systems via single term Walsh series approach", *Int. J. Syst. Sci.*, vol. 12, no. 4, 1981, pp. 443-454.

[71] K. R. Palanisamy and R. G. Prasada, "Optimal control of linear systems with delays in state and control via Walsh functions", *IEE Proc-D*, vol. 130, no. 6, 1983, pp. 300-312.

[72] H. T. Pedro, M. H. Kobayashi, J. M. Pereira, and C. F. Coimbra, "Variable order modeling of diffusive-convective effects on the oscillatory flow past a sphere", *J. Vib. Control*, vol. 14, no. 9-10, 2008, 1659-1672.

[73] K. Rabiei, Y. Ordokhani, and E. Babolian, "Numerical Solution of 1D and 2D fractional optimal control of system via Bernoulli polynomials", *Int. J. Appl. Comput. Math.*, vol. 4, no. 1, 2018, pp. 1-17.

[74] Z. Rafiei, B. Kafash, and S. M. Karbassi, "A new approach based on using Chebyshev wavelets for solving various optimal control problems", *Comput. Appl. Math.*, vol. 37, no. 1, 2018, pp. 144-157.

[75] P. Rahimkhani, Y. Ordokhani, and E. Babolian, "Fractional-order Bernoulli wavelets and their applications", *Appl. Math. Model.*, vol. 40, no. 17-18, 2016, pp. 8087-8107.

[76] P. Rahimkhani, Y. Ordokhani, and E. Babolian, "An efficient approximate method for solving delay fractional optimal control problems", *Nonlinear Dynam.*, vol. 86, no. 3, 2016, pp. 1649-1661.

[77] P. Rahimkhani, Y. Ordokhani, and E. Babolian, "Müntz-Legendre wavelet operational matrix of fractional-order integration and its applications for solving the fractional pantograph differential equations", *Numer. Algorithms*, vol. 77, no. 4, 2018, pp. 1283-1305.

[78] P. Rahimkhani and Y. Ordokhani, "Generalized fractional-order Bernoulli-Legendre functions: an effective tool for solving two-dimensional fractional optimal control problems", *IMA J. Math. Control I.*, vol. 36, no. 1, 2019, pp. 185-212.

[79] P. Rahimkhani and Y. Ordokhani, "Numerical investigation of distributed-order fractional optimal control problems via Bernstein wavelets", *Optim. Contr. Appl. Met.*, vol. 42, no. 1, 2021, pp. 355-373.

[80] S. A. Rakhshan and S. Effati, "Fractional optimal control problems with time-varying delay: A new delay fractional Euler–Lagrange equations", *J. Frankl. Inst.*, vol. 357, no. 10, 2020, pp. 5954-5988.

[81] S. A. Rakhshan, S. Effati, and A. Vahidian Kamyad, "Solving a class of fractional optimal control problems by the Hamilton-Jacobi-Bellman equation", *J. Vib. Control*, vol. 24, no. 9, 2018, pp. 1741-1756.

[82] L. E. Ramirez and C. F. Coimbra, "On the variable order dynamics of the nonlinear wake caused by a sedimenting particle", *Physica D: nonlinear phenomena*, vol. 240, no. 13, 2011, 1111-1118.

[83] Y. A. Rossikhin and M. V. Shitikova, "Applications of fractional calculus to dynamic problems of linear and nonlinear hereditary mechanics of solids", 1997, pp. 15-67.

[84] S. Sabermahani, Y. Ordokhani, and S. A. Yousefi, "Fractional-order Lagrange polynomials: an application for solving delay fractional optimal control problems", *T. I. Meas. Control*, vol. 41, no. 11, 2019, pp. 2997-3009.

[85] J. Sabouri, S. Effati, and M. Pakdaman, "A neural network approach for solving a class of fractional optimal control problems", *Neural Process. Lett.*, vol. 45, no. 1, 2017, pp. 59-74.

[86] H. Saeedi, M. M. Moghadam, N. Mollahasani, and G. N. Chuev, "A CAS wavelet method for solving nonlinear Fredholm integro-differential equations of fractional order", *Commun. Nonlinear Sci.*, vol. 16, no. 3, 2011, pp. 1154-1163.

[87] E. Safaie and M. H. Farahi, "An approximation method for numerical solution of multi-dimensional feedback delay fractional optimal control problems by Bernstein polynomials", vol. 4, no. 1, 2014, pp. 77-94.

[88] E. Safaie, M. H. Farahi, and M. F. Ardehaie, "An approximate method for numerically solving multi-dimensional delay fractional optimal control problems by Bernstein polynomials", *Comput. Appl. Math.*, vol. 34, no. 3, 2015, pp. 831-846.

[89] E. Safaie and M. H. Farahi, "An approximate method for solving fractional TBVP with state delay by Bernstein polynomials", *Adv. Differ. Equ-Ny.*, vol. 2016, no. 1, 2016, pp. 1-16.

[90] P. K. Sahu and S. Saha Ray, "Comparison on wavelets techniques for solving fractional optimal control problems", *J. Vib. Control*, vol. 24, no. 6, 2018, pp.1185-1201.

[91] S. G. Samko and B. Ross, "Integration and differentiation to a variable fractional order", *Integr. Transf. Spec. F.*, vol. 1, no. 4, 1993, pp. 277-300.

[92] T. Sandev, A. V. Chechkin, N. Korabel, H. Kantz, I. M. Sokolov, and R. Metzler, "Distributed-order diffusion equations and multifractality: models and solutions", *Phys. Rev. E*, vol. 92, no. 4, 2015, pp. 042117.

[93] J. J. Shyu, S. C. Pei, and C. H. Chan, "An iterative method for the design of variable fractional-order FIR differintegrators", *Signal Process.*, vol. 89, no. 3, 2009, pp. 320-327.

[94] N. Singha and C. Nahak, "An efficient approximation technique for solving a class of fractional optimal control problems", *J. Optimiz. Theory App.*, vol. 174. no. 3, 2017, pp. 785-802.

[95] I. Sokolov, A. Chechkin, and J. Klafter, "Distributed-order fractional kinetics", *Acta Phys. Pol. B*, vol. 35, 2004, pp. 1323–1341.

[96] H. G. Sun, W. Chen, H. Wei, and Y. Q. Chen, "A comparative study of constant-order and variable-order fractional models in characterizing memory property of systems", *The European Physical Journal Special Topics*, vol. 193, no. 1, 2011, pp. 185-192.

[97] D. Y. Sun and T. C. Huang, "The solutions of time-delayed optimal control problems by the use of modified line-up competition algorithm", *J. Taiwan Inst. Chem. E.*, vol. 41, no. 1, 2010, pp. 54-64.

[98] N. H. Sweilam and T. M. Al-Ajami, "Legendre spectral-collocation method for solving some types of fractional optimal control problems", *J. Advanc. Res.*, vol. 6, no. 3, 2015, pp. 393-403.

[99] P. T. Toan, T. N. Vo, and M. Razzaghi, "Taylor wavelet method for fractional delay differential equations", *Eng. Comput.*, 2020, pp. 1-12.

[100] L. N. Trefethen, "Approximation Theory and Approximation Practice", *Society for Industrial and Applied Mathematics*, USA.

[101] F. Valian, Y. Ordokhani, and M.A. Vali, "Numerical Solution of Fractional Optimal Control Problems with Inequality Constraint Using the Fractional-Order Bernoulli Wavelet Functions", *IJST-T. Electr. Eng.*, vol. 44, no. 4, 2020, pp. 1513-1528.

[102] P. Vichitkunakorn, T. N. Vo, and M. Razzaghi, "A numerical method for fractional pantograph differential equations based on Taylor wavelets", *T. I. Meas. Control*, vol. 42, no. 7, 2020, pp. 1334-1344.

[103] X. T. Wang, "Numerical solutions of optimal control for time delay systems by hybrid of block-pulse functions and Legendre polynomials", *Appl. Math. Comput.*, vol. 184, no. 2, 2007, pp. 849-856.

[104] Y. Wang and Q. Fan, "The second kind Chebyshev wavelet method for solving fractional differential equations", *Appl. Math. Comput.*, vol. 218, no. 17, 2012, pp. 8592-8601.

[105] X. Xu, L. Xiong, and F. Zhou, "Solving fractional optimal control problems with inequality constraints by a new kind of Chebyshev wavelets method", *J. Comput. Sci-Neth.* vol. 54, 2021, pp. 101412.

[106] A. Yari, "Numerical solution for fractional optimal control problems by Hermite polynomials", *J. Vib. Control*, vol. 27, no. 5-6, 2020, pp. 698-716.

[107] W. Yonthanthum, A. Rattana, and M. Razzaghi, "An approximate method for solving fractional optimal control problems by the hybrid of block-pulse functions and Taylor polynomials", *Optim. Contr. Appl. Met.*, vol. 39, no. 2, 2018, pp. 873-887.

[108] B. Yuttanan and M. Razzaghi, "Legendre wavelets approach for numerical solutions of distributed order fractional differential equations", *Appl. Math. Model.*, vol. 70, 2019, pp. 350-364.

[109] B. Yuttanan, M. Razzaghi, and T.N. Vo, "A fractional-order generalized Taylor wavelet method for nonlinear fractional delay and nonlinear fractional pantograph differential equations", *Math. Method. Appl. Sci.*, vol. 44, no. 5, 2021, pp. 4156-4175.

[110] M. A. Zaky, "A Legendre collocation method for distributed-order fractional optimal control problems", *Nonlinear Dynam.*, vol. 91, no. 4, 2018, pp. 2667-2681.

[111] S. S. Zeid and M. Yousefi, "Approximated solutions of linear quadratic fractional optimal control problems", *J. Appl. Math. Stat. Info.*, vol. 12, no. 2, 2016, pp. 83-94.